Journal of Hydrology 548 (2017) 754–769

Contents lists available at ScienceDirect

Journal of Hydrology

journal homepage: www.elsevier.com/locate/jhydrol

Research papers

Geology and geomorphology control suspended sediment yield and modulate increases following timber harvest in temperate headwater streams

Sharon Bywater-Reyes *, Catalina Segura, Kevin D. Bladon

Department of Forest Engineering, Resources, and Management, College of Forestry, Oregon State University, Corvallis, OR 97331, USA

ARTICLE INFO

Article history:
Received 20 August 2016
Received in revised form 23 March 2017
Accepted 24 March 2017
Available online 28 March 2017
This manuscript was handled by Tim R. McVicar, Editor-in-Chief, with the assistance of Patrick N. Lane, Associate Editor

Keywords:
Sediment transport
Paired watershed study
Lithologic control
Physiographic characteristics
Mountain streams
Pacific Northwest

ABSTRACT

Suspended sediment transport is an important contributor to ecologic and geomorphic functions of streams. However, it is challenging to generalize predictions of sediment yield because it is influenced by many factors. In this study, we quantified the relevance of natural controls (e.g., geology, catchment physiography) on suspended sediment yield (SSY) in headwater streams managed for timber harvest. We collected and analyzed six years of data from 10 sites (five headwater sub-catchments and five watershed outlets) in the Trask River Watershed (western Oregon, United States). We used generalized least squares regression models to investigate how the parameters of the SSY rating curve varied as a function of catchment setting, and whether the setting modulated the SSY response to forest harvesting. Results indicated that the highest intercepts (α) of the power relation between unit discharge and SSY were associated with sites underlain primarily by friable rocks (e.g., sedimentary formations). The greatest increases in SSY after forest harvesting (up to an order of magnitude) also occurred at sites underlain by the more friable lithologies. In contrast, basins underlain by resistant lithologies (intrusive rocks) had lower SSY and were more resilient to management-related increases in SSY. As such, the impact of forest management activities (e.g., use of forested buffers; building of new roads) on the variability in SSY was primarily contingent on catchment lithology. Sites with higher SSY, or harvest-related increases in SSY, also generally had a) lower mean elevation and slope, b) greater landscape roughness, and c) lower sediment connectivity. We used principal component analysis (PCA) to further explore the relationship between SSY and several basin physiographic variables. The PCA clearly separated sites underlain by friable geologic units from those underlain by resistant lithologies. Results are consistent with greater rates of weathering and supply of sediment to headwater streams in catchments with more friable lithologies, and limited sediment supply in catchments underlain by resistant lithologies. We hypothesize that a similar framework may aid in predicting the overall SSY of a catchment as well as its susceptibility to increases in SSY following forest harvesting.

1. Introduction

Mountainous headwater streams may disproportionally contribute to global sediment discharge (Kao and Milliman, 2008; Milliman et al., 1999; Milliman and Syvitski, 1992), particularly if impacted by land-use practices that often increase fine sediment transport and deposition (Binkley and Brown, 1993; Croke and Hairsine, 2006; Gomi et al., 2005; Montgomery, 2007; Sofia et al., 2016; Tarolli and Sofia, 2016). Fine sediment can negatively impact fishes and other aquatic ecosystem elements (Kemp et al., 2011; Suttle et al., 2004) and degrade water quality (Brown and Binkley, 1994; Wood and Armitage, 1997). It is, therefore, considered a pollutant under the United States (US) Clean Water Act. In the western US, where mountainous regions of the temperate Pacific Northwest (PNW) are targeted for timber harvesting activities, the Environmental Protection Agency has classified >70% of streams as water-quality impaired—~19,000 km of streams are threatened by sediment pollution in Oregon alone (United States Environmental Protection Agency, 2016). Despite this, Total Maximum Daily Loads (TMDLs) for suspended sediment have not been defined in many states, including Oregon. As such, deciphering the relative controls on suspended sediment transport in mountainous headwater streams may be particularly crucial for understanding both local effects important for water quality standards in

* Corresponding author.
E-mail address: bywaters@oregonstate.edu (S. Bywater-Reyes).

http://dx.doi.org/10.1016/j.jhydrol.2017.03.048
0022-1694/

timber-dependent economies (Haynes, 2003; Prestemon et al., 2015) as well as mass flux of material on a broader scale.

In an effort to quantify the impact of forest practices on fine sediment dynamics in temperate headwater catchments, an early paired-watershed study (Alsea Watershed Study in Oregon) compared 1960's forest harvesting practices that included clearcutting and burning of slash to forest management practices that retained riparian vegetation along streams as buffers (Beschta, 1978; Brown and Krygier, 1971). This study became the prime example of the environmental consequences of unregulated logging, as annual sediment yields increased up to 500% in the more heavily disturbed catchment (Beschta, 1978). In part based of these findings, contemporary forest management practices now limit slash burning, harvest size, and harvest frequency, while requiring riparian buffers to be retained around streams (e.g., Oregon's Forest Protection Laws). The principal objectives of these regulations is to mediate increased sediment yields to streams and regulate stream temperatures. A number of paired-watershed studies have since occurred to assess the efficacy of *modern* forest practices on limiting suspended sediment yields (SSY). The conclusions of these studies have been mixed (Binkley and Brown, 1993; Gomi et al., 2005) showing increases (i.e., Macdonald et al., 2003), decreases (i.e., Grant and Wolff, 1991), and no changes (i.e., Hotta et al., 2007) in SSY, hindering generalization concerning controls on sediment flux rates in catchments impacted by contemporary forest management activities.

The impacts of land-management on SSY are generally a function of both sediment supply and transport capacity. However, thresholds for fine-sediment motion are met frequently in most systems, often rendering sediment supply the limiting factor (Church, 2002; Paustian and Beschta, 1979). Sediment supply generally varies across landscapes depending on factors associated with catchment setting, such as climate, physiography, and geology, or disturbance history (Buss et al., 2017; Croke and Hairsine, 2006; Gomi et al., 2005; Hicks et al., 1996; Johnstone and Hilley, 2014; Montgomery, 1999; Montgomery and Brandon, 2002; O'Byrne, 1967; O'Connor et al., 2014). For instance, SSY was greater in more erodible (e.g., sedimentary and volcanics) lithologies compared to more resistant lithologies in Western Oregon and northwestern California (Wise and O'Connor, 2016), the Idaho Rocky Mountains (Mueller et al., 2016; Mueller and Pitlick, 2013), Wyoming (Colby et al., 1956), and in New Zealand (Hicks et al., 1996). However, following high severity disturbances like wildfire, the potential role of lithology may be greatly reduced relative to the fine-sediment supply associated with the disturbance (Moody et al., 2008; Wise and O'Connor, 2016).

Factors such as physiography and land management affect SSY, but the relative influence of these in relation to other controls is less clear. In a global analysis of large rivers, Syvitski and Milliman (2007) found that geologic and physiographic variables explained the majority of variance in long-term SSY among sites (65%), whereas climate and land use accounted for 14% and 16%, respectively. In a setting of uniform lithology, Klein et al. (2012) found that harvest intensity and drainage area best predicted 10% turbidity exceedance levels (indicative of chronic turbidity), whereas physiographic variables did not improve the prediction. For Washington streams draining managed forests of the PNW, turbidity (a proxy for suspended sediment transport) was correlated with geologic province, independent of forest management practices (Reiter et al., 2009). Thus, evidence suggests that both basin characteristics (lithology and physiographic conditions) and land management influence SSY. Furthermore, interdependencies between catchment setting and the response of SSY to land management activities may exist. For example, in North Westland catchments of New Zealand, O'Loughlin and Pearce (1976) found the most substantial increases in SSY occurred following forest removal in catchments underlain by easily erodible sedimentary formations.

The purpose of this research was to examine the relative influence of basin setting (lithology and basin physiographic variables) and forest management on SSY in temperate headwater catchments. Specifically, we analysed 6 years of data from a watershed, which included harvested and unharvested sub-catchments and was underlain by heterogeneous lithologies, to achieve the following objectives:

1. Quantify how suspended sediment yield varies by catchment setting in forested headwater catchments;
2. Determine whether contemporary forest management practices impact annual suspended sediment yield in forested headwater catchments;
3. Determine whether there are natural catchment settings that result in different levels of vulnerability or resilience to increases in suspended sediment yield associated with disturbances (e.g., harvest activities).

These objectives provide the structural subheadings used in the following Methods, Results, and Discussion sections.

2. Background

2.1. Trask River Watershed Study

We used data from the the Trask River Watershed Study (TRWS) of Oregon's Watersheds Research Cooperative (WRC; http://watershedsresearch.org/). The WRC studies were established to investigate the impact of contemporary forest management practices on biological, chemical, and physical water quality, including fine-sediment transport. TRWS is located in the northern Oregon Coast Range, occupying ~25 km^2 on the East Fork South Fork Trask River in the Wilson-Trask-Nestucca Watershed, which drains to the Pacific Ocean at Tillamook Bay (Fig. 1). The TRWS used a nested, paired-watershed approach. The study area is composed of four larger catchments: Pothole (PH), Gus Creek (GC), Upper Main (UM), and Rock Creek (RCK), with each encompassing several smaller sub-catchments (Fig. 1). Three of these larger catchments (PH, GC, and UM) included harvested sub-catchments, while one catchment (RCK) remained unharvested as a reference (Table 1). We used data from 10 sites, which had continuous records of discharge and suspended sediment across the period of interest, including five headwater sub-catchments and five watershed outlets.

Baseline data collection began in water year 2010 and continued through water year 2015, with road upgrades (July–August 2011) and harvest (May–November 2012) occurring in the middle of the study period. In particular, new roads were built July through August 2011 in the UM (UM1 and UM2) and GC (GC3) watersheds (Table 1). No new roads were built in the PH watershed; however, upgrades on existing roads occurred throughout the TRWS (August 2011). Road densities were similar for all watersheds, with UM2 and GC3 having slightly higher densities (Table 1). Harvest treatments of study sub-watersheds consisted of clearcuts (UM2 and GC3) and a clearcut with buffers (50 ft; ~15 m; PH4) that were conducted May–November 2012. Depending on the slope, headwater sub-catchments were harvested using different contemporary techniques, including ground-based and cable logging (Table 1).

Forests in the TRWS are dominated by second-growth Douglas-fir (*Pseudotsuga menziesii*), with populations of red alder (*Alnus rubra*) primarily located in riparian areas. The entire watershed has been subjected to a combination of historic fires (Tillamook

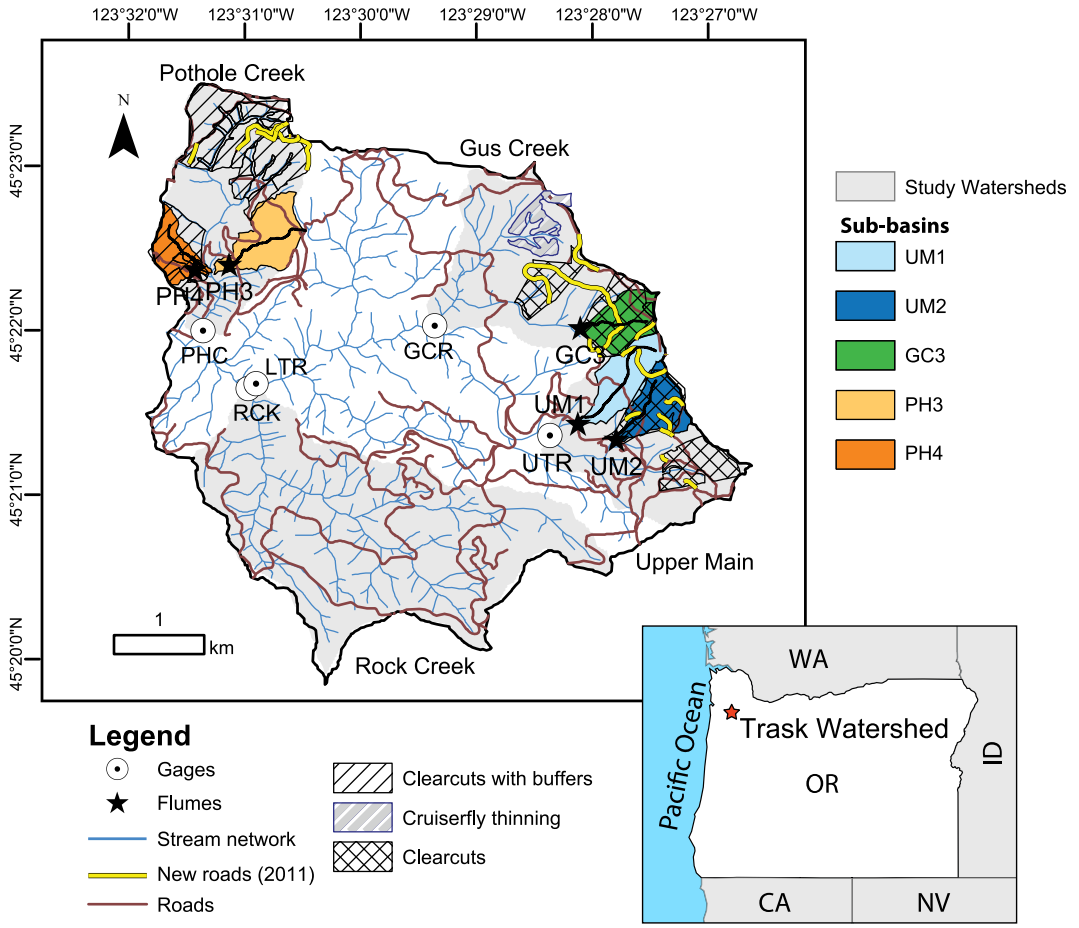

Fig. 1. Trask River Watershed Study location showing treatment (Pothole, Gus, and Upper Main) and reference (Rock Creek) watersheds and nested headwater catchments (numbered). Suspended sediment and discharge data were collected at sub-basin (flumes) and watershed (gages) outlets. New roads were built in summer 2011 and forest harvest was conducted within headwater catchments in summer 2012.

Table 1
Sub-catchment characteristics showing physiographic variables and treatment details.

Catchment	Slope (%)[1]	Relief (m)[1]	Channel Slope (%)[1]	Stream Morphology[2]	Dominant Lithology[3]	Harvest Type	% Area Harvested	Existing Roads (m)	New Roads (m)	Total Road Density (m/m^2)	Harvest Type[4]
UM1	19.7	317	22	step-pool	Intrusive	No Harvest	0	776	564	0.0030	NA
UM2	17.3	274	26	step-pool	Sedimentary	Clearcut	83	838	904	0.0046	Ground
GC3	21.9	321	27	step-pool/cascade	Intrusive	Clearcut	94	754	918	0.0044	Cable
PH3	20.1	285	17	step-pool	Landslide sediments	No Harvest	0	1477	NA	0.0030	NA
PH4	18.5	229	22	pool-riffle/ step-pool	Sedimentary	Clearcut with Buffers	92	817	NA	0.0031	Ground

[1] Derived from LiDAR (Oregon Lidar Consortium, 2012).
[2] From Turner et al. (2007).
[3] Wells et al. (1994).
[4] Dominant method by percent catchment area.

Fires, 1933–1951 and older complexes; Zybach, 2003) and timber harvest activities, resulting in complete removal of old growth timber in the region. The TRWS is representative of temperate forested regions (e.g., PNW), with climate heavily influenced by air masses sourced from the Pacific Ocean—this results in high annual precipitation (~215 cm year^{-1} during the study period; Fig. 2) falling predominantly as rainfall during the winter (November–January). During the study period, median annual discharge and cumulatlive annual precipitation varied—water years 2010, 2011, and 2013 were higher, whereas 2014 and 2015 were lower (Fig. 2). The onset of below-average, drought conditions was evident in water years 2014 and 2015 (Fig. 2).

The study watersheds are located within the Coastal Range geologic province of western Oregon. Because of the geologic history of the region, the underlying lithology varies throughout the TRWS (Figs. 3A; 4 and Table 2). The oldest geologic units within the basin are associated with accretion of the Siletz terrane, which forms the basement of the Oregon Coast Range. The associated Siletz River Volcanics (Paleocene to Middle Eocene) are composed mostly of sea-floor basalt flows deposited on the former margin of the coast

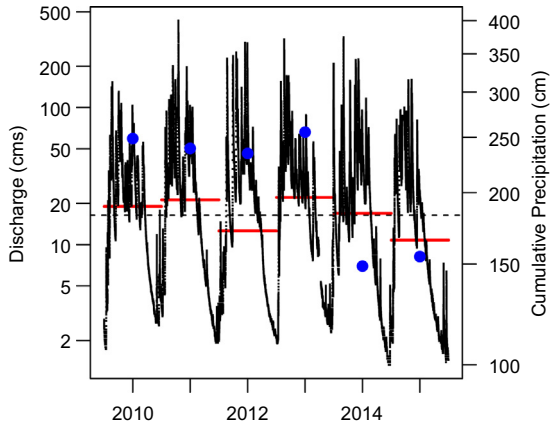

Fig. 2. Hydrograph for USGS Site No. 14302480 Trask River above Cedar Creek (representative of the region; continuous record for the period of interest), downstream of study watershed for the period of study. Red line = median annual discharge; dashed line = median discharge for the period of record; blue dots = cumulative annual precipitation (onset of drought in water year 2014).

prior to accretion (Miller, 2014). The Tillamook Volcanics (Middle Eocene) were similarly deposited in a marine environment, but contain more reworked flows (tuffs, volcaniclastic breccias). Intrusive rocks associated with the Tillamook Volcanics include a diabase unit and basaltic dikes and sills (USGS, 2014). Marine sedimentary rocks were deposited atop the Siletz terrane, including the Eocene Trask River (turbidite deposits) and Yamhill formations (Miller, 2014; USGS, 2014; Wells et al., 1994). In general, the eastern study catchments (e.g., UM1, UM2, UTR, GC3, GCR) are composed of resistant diabase, whereas the western catchments (i.e., PH3, PH4, PHC, RCK, LTR) have larger proportions of volcanic and sedimentary formations and landslide deposits (Fig. 4).

Basin characteristics (catchment slope, channel slope, and stream morphology; Table 1) vary throughout TRWS catchments as a function of the lithologic setting (Fig. 3A). Limited soil information indicates the dominant soil type is roughly correlated with lithology; however, most soils are well-drained loams to gravelly loams with high water saturated hydraulic conductivity. Siletz Volcanics are associated with medial loam to very gravelly medial loam of the Hemcross-Klistan complex. Most of the remainder of the watershed is composed of medial loam to very cobbly loam soil of the Murtip-Caterl-Laderly complex. Within the PH watershed, low saturated hydraulic conductivity have been documented (Soil survey of Tillamook County, Oregon, 2013). Soil erodibility (K factor from the Universal Soil Loss Equation; USLE) and thickness vary as a function of lithology, with the lowest K factor and thinnest soils in the northeast portion of Trask, which is underlain by diabase (Schwarz and Alexander, 1995).

Certain regions of the TRWS display landslide features (Fig. 3B), with the most prominent complexes in the UM and PH watersheds. In particular, both unharvested (reference) headwater subcatchments (UM1, PH3) display a predominance of scarp and slump terrain or a large proportion of landslide deposits (Fig. 4). However, while the UM watershed displays the characteristic "hour-glass" shape of a shallow earthflow, the PH catchment appears to be a rotational slump-earth complex (Highland and Bobrowsky, 2008). Volcaniclastic formations of western Oregon, including those within the Yamhill Formation, are linked to landside hazards (Burns et al., 2006; Marshall, 2016; Wong, 1999).

2.2. Suspended sediment and discharge measurements

Headwater catchments and downstream watershed outlets were instrumented to record stream stage and collect water samples for suspended sediment concentration (Fig. 1). These data were used to derive discharge and SSY (expressed as sediment discharge per unit discharge per unit area). Headwater sites were outfitted with Montana flumes, whereas a stage-discharge rating curve approach was used at downstream sites (gages). Water samples were collected at all sites with automatic water samplers (Teledyne ISCO 3700) on a daily basis (12- to 24-h interval) for the upstream catchments and based on a turbidity threshold sampling scheme for downstream sites (Lewis and Eads, 2009). The threshold-based scheme resulted in samples collected only during storm events. All water samples were filtered using 1.5 μm glass fiber filter paper (Whatman 934-AH), dried, and weighed following standard protocols (Redwood Sciences Laboratory, 2016).

Given the discrepancy between sampling protocols among headwater and downstream sites, we only included samples collected during storms across all sites. We defined a storm event as being preceded by 24 h without precipitation and having a magnitude of at least 40 mm based on the precipitation record from two climate stations (Fig. 1). This threshold was found to most consis-

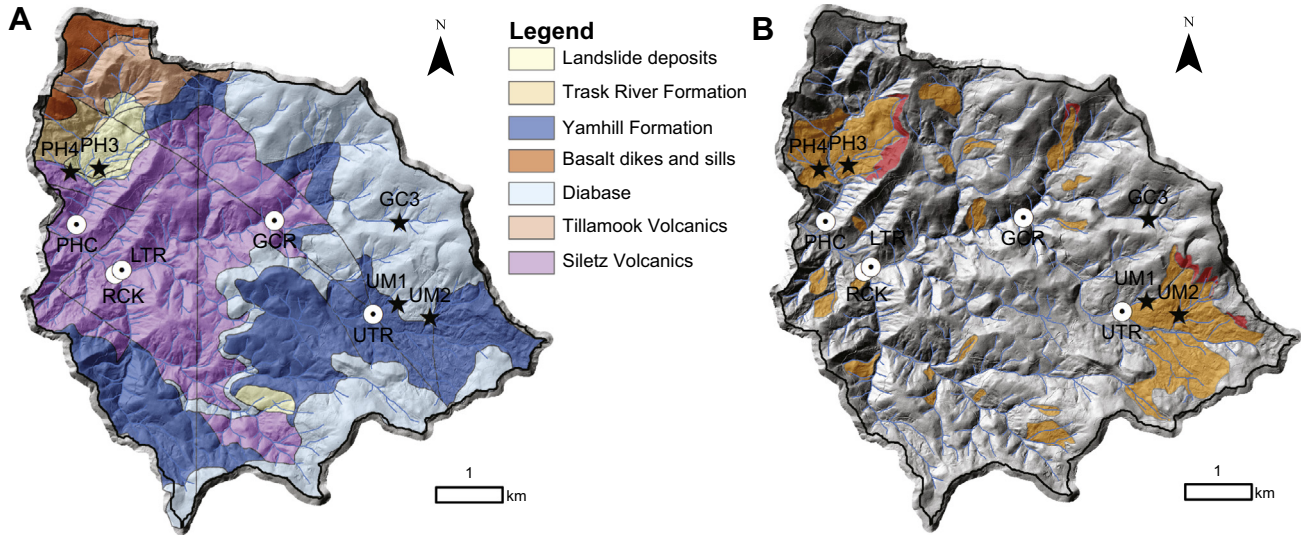

Fig. 3. Maps of geology (A; Wells et al., 1994) and areas characterized by mass wasting (B; scarps in red and slump flow in orange (Turner et al., 2007) across the TRWS.

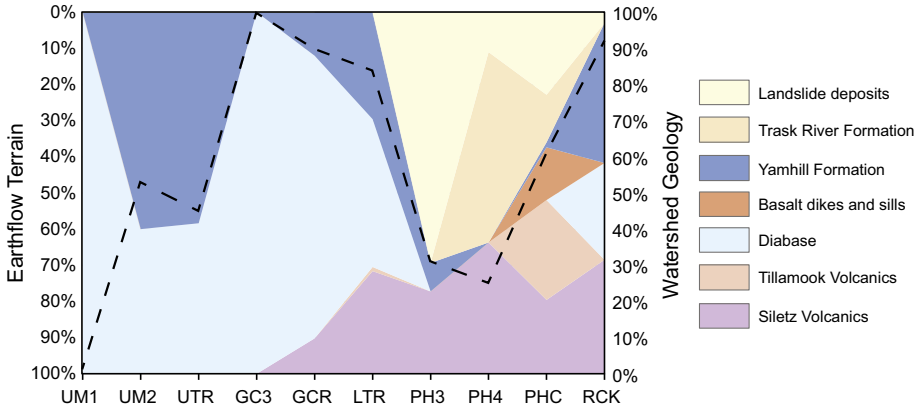

Fig. 4. Percent of catchment area with earthflow terrain (dashed line), principally scarps and slumps (Turner et al., 2007) and percent of catchment area composed of different geologic units (colored areas; Wells et al., 1994). Generally ordered by watershed (starting with same letter) from upstream (numbered) to downstream for each. See Figs. 1 and 3 for locations.

Table 2
Catchment area and percent geologic unit per watershed in the TRWS varies.

Catchment	Area (ha)	*Catchment Geology (% Area)*[1]							% Friable[2]
		Siletz	Tillamook	Diabase	Dikes/Sills	Yamhill	Trask River	Landslide	
UM1	44.5	0	0	100	0	0	0	0	0
UM2	37.6	0	0	40	0	60	0	0	0
UTR	278.8	0	0	42	0	58	0	0	0
GC3	37.8	0	0	100	0	0	0	0	0
GCR	302.2	10	0	78	0	12	0	0	10
LTR	1458.9	28	1	41	0	30	0	0	28
PH3	48.5	23	0	0	0	8	0	69	92
PH4	26.4	36	0	0	0	0	52	11	99
PHC	324.6	20	28	0	15	1	13	23	56
RCK	667.6	32	0	27	0	39	0	3	35

[1] Calculated from digitized version of Wells et al. (1994) in ESRI ArcGIS 10.2.2.
[2] % Catchment area underlain by lithologies positively correlated (see Table 4) to site-dependent SSY.

tently identify storms (92 total) represented by both sample collection schemes.

2.3. Rating curve theoretical background

The relationship between suspended sediment yield (SSY) and unit discharge (Q) was described with a power function (Eq. (1)) that can also be expressed in a linear form (Eq. (2)):

$$Q_s = \alpha Q^{\beta} \quad (1)$$

$$\log(Q_s) = \beta \log(Q) + \log \alpha \quad (2)$$

where Q_s is SSY (kg ha^{-1} h^{-1}), Q is unit water discharge (m^3 ha^{-1} h^{-1}), and α and β are empirically derived parameters that vary across catchments (Hotta et al., 2007; Roman et al., 2012; Syvitski et al., 2000). The α parameter is considered a metric of erosion severity whereas the β parameter is a function of the erosive power of a stream (Desilets et al., 2007), with larger values indicating new sources of sediment availability at higher Q (Sheridan et al., 2011). Both Q_s and Q were normalized by drainage area to account for differences in catchment contributing areas, allowing for unbiased comparison among sites (Leopold et al., 1964; Milliman and Meade, 1983). The linearized function (Eq. (2)) was used in linear statistical models to investigate how the equation parameters (α and β) varied by site (objective 1) and year (objective 2).

Changes in either discharge or sediment supply can alter the rating curve parameters (α and β; Warrick and Rubin, 2007). For example, if sediment supply increased but discharge stayed the same, the rating curve α coefficient would increase (Warrick and Rubin, 2007). On the other hand, if discharge increased but sediment supply remained constant, α would decrease because of dilution (Warrick and Rubin, 2007). When watersheds are harvested, streamflow may increase because of a reduction in evapotranspiration (Macdonald et al., 2003; Surfleet and Skaugset, 2013). Changes in discharge can alter SSY rating curve relations (Warrick and Rubin, 2007). Thus, any detected harvest-related increases in sediment supply would have to be greater than the associated discharge dilution effect.

3. Methods

3.1. Suspended sediment yield by catchment setting

To address objective 1, we tested for site differences in the relationship between SSY and catchment setting (geology and physiography) by quantifying the parameters of Eq. (2) using sediment yields from all 10 sites (all-site analysis; statistical analysis 1A) in generalized least squares candidate models. These models were developed to predict $\log(Q_s)$ using site (proxy for catchment setting) and $\log(Q)$, or an interaction between the two, as fixed factors. To account for intra-year variance, we included water year both with and without interactions between site and $\log(Q)$ (statistical analysis 1A; Zuur et al., 2009). Model selection from candidate models was based on an Akaike Information Criterion (AIC) (Akaike, 1974) corrected for small sample size (AICc), where plausible models have ΔAICc < 4 (Burnham and Anderson, 2002). To test the robustness of the all-site analysis and characterize the behavior of the rating curve at the treatment watersheds, we

repeated the procedure outlined for the all-site analysis including only the five headwater sub-catchments (statistical analysis 1B).

All statistical analyses were performed in R version 3.1.1 (R Development Core Team, 2015). The AICcmodavg package was used for AICc analysis (Mazerolle, 2015). The lme4 package was used for mixed effect model (generalized least squares) analysis (Bates et al., 2015). The effects and LMERConvenienceFunctions packages (Tremblay, 2015) were used to compute an "effect" as the range in the response variable resulting from varying the predictor of interest over its observed range while holding all others constant at the midpoint of their observed range. We adopt this definition of an effect in this study. Standard errors and confidence limits for the effect(s) were calculated assuming a normal distribution.

3.2. Forest management effects on suspended sediment yield

To address objective 2, we quantified the effect of forest management activities (road upgrades in summer 2011 and timber harvest in summer 2012) on SSY by quantifying year-to-year changes in rating curve parameters (Eq. (2)) for harvested, headwater catchments. We did not conduct this analysis on downstream sites because of the confounding effects of multiple treatments within each watershed (Fig. 1). To test how $\log(Q_s)$ varied by water year, we constructed generalized least squares candidates by specifying water year or water year with a site interaction as a fixed factor. To account for the variance caused by $\log(Q)$ and site we included $\log(Q)$, site, or an interaction between $\log(Q)$ and site as random factors (statistical analysis 2). As with the other analyses, we chose the most parsimonious model based on the AICc.

3.3. Catchment setting and physiographic variables

3.3.1. Catchment physiographic variables as proxies for geomorphic processes

Objective 3 was to determine whether catchment setting influenced the vulnerability or resilience of catchments to increases in SSY associated with forest harvest. To achieve this objective, catchment geologic and physiographic parameters were examined as potential explanatory variables for observed SSY results (described in Sections 3.1 and 3.2). Several physiographic variables were considered for the five harvested, upstream sites based on the expectation that they may vary as a function of dominant geomorphic processes operating within small watersheds (Table 1). Generated metrics included the distributions of elevation (hypsometry), slope, a landscape roughness metric (topographic position index), and an index of sediment connectivity.

Catchment hypsometry (relationship between elevation and area) reflects the tectonic, climatic, and erosional history of a catchment (Cooley, 2015; Langbein, 1947; Strahler, 1952). Change in elevation (slope) is correlated with slope stability (e.g., Carson, 1976) and stream morphology (e.g., Montgomery and Buffington, 1997), and is a proxy for the energy available to transport sediment (Whipple and Tucker, 1999; Wobus et al., 2006). Landscape roughness indices are correlated with landslide type and activity (Booth et al., 2013, 2009; McKean and Roering, 2004), stream morphology (Cavalli et al., 2008; McKean et al., 2009), and soil/sedimentary thickness (Pelletier et al., 2016)—in this study, landscape roughness was used as a proxy for sediment availability. As an indicator of roughness, we used the standardized topographic position index (SD TPI), a metric of variation in elevation at a location relative to its neighbors' position (Cooley, 2015; Jenness et al., 2013). A radius of 10 m was used as it was found to identify within network roughness features (of interest here) as compared to network (ridge and valley) scale features—this analysis was performed using the Land Facet Corridor Tools extension version 1.2.605 (Jenness et al., 2013; Majka et al., 2007). The index of sediment connectivity (IC), which indicates areas likely to experience storage (low relative values) versus transport (high relative values) (Borselli et al., 2008; Cavalli et al., 2013; Tarolli and Sofia, 2016), was calculated using the SedInConnect tool (Cavalli et al., 2013; Crema et al., 2015). Metrics were derived from a high-resolution (3 ft; 0.9 m) LiDAR bare-earth raster (Oregon Lidar Consortium, 2012) in ArcGIS 10.2.2 (ESRI, Redlands, CA), unless otherwise indicated.

3.3.2. Physiographic variable analysis

The distributions of each physiographic variable were visually explored with histograms and empirical cumulative distribution functions for each site—the first four moments (mean, variance, skewness, and kurtosis) of the distributions were quantified for each. Based on this preliminary exploration, moments of variables with the greatest differences or groupings among sites were included in a principal component analysis (PCA; statistical analysis 3) that reduced the dimensionality of many variables into principal components comprised of linear combinations of the variables (Legendre and Legendre, 1998). Based on the proportion of explained variance, we retained principal components (PCs) for interpretation, dismissing components after 90% of the variance was reached. Larger component loadings (analogous to correlation coefficients) within a PC indicate a large proportion of variance explained by a variable. A large loading was defined as anything greater than expected if all variables contributed equally to the observed variance. The scores for each site were interpreted in the context of their location (score) in the new, rotated ordination space using distance biplots, which also revealed the impact variables had on sample location (Legendre and Legendre, 1998). We identified site differences or similarities using this procedure, and explored the importance of the physiographic variables responsible for these patterns. This analysis was completed using the *prcomp* function in R version 3.1.1 (R Development Core Team, 2015) after centering and scaling variables. The mean of variables centered at zero (i.e., SD TPI) were excluded from the analysis.

4. Results

4.1. Suspended sediment transport by catchment setting

The generalized least squares regression model analysis indicated that suspended sediment yield, SSY (Q_s), was a function of site when we accounted for year-to-year variability (Fig. 5A,B; Table A1). Both the intercept (α) and slope (β) of the Q_s – Q rating curve were a function of site, as indicated by the site-Q interaction (Table A1). The disparity in suspended sediment sampling methods (time interval for upstream sites versus turbidity-threshold method for downstream sites) led to a slope parameter (β) bias, with steeper slopes generally observed at the turbidity-threshold sites (downstream sites) (Table A1). For this reason, a comparison of absolute β parameter values among all sites was not possible. However, the α and β were weakly negatively correlated ($r = -0.47$). Results from the analysis conducted on the upstream sites in isolation (Figs. 6; 7; Table A2) were consistent with the all-site analysis (statistical analysis 1A and 1B).

To avoid the method's bias and generalize across sites, we present site-dependent SSY, where SSY is Q_s calculated if with other parameters held constant at the midpoint of their range (Figs. 5C and 7C). SSY varied over an order-of-magnitude between some sites (Fig. 5C). Sites within the PH catchment (PH3, PH4) had the largest SSY, with ~3.8- to 6.9-times greater rates than sites located within the UM and GC catchments (Fig. 5C; Table 3).

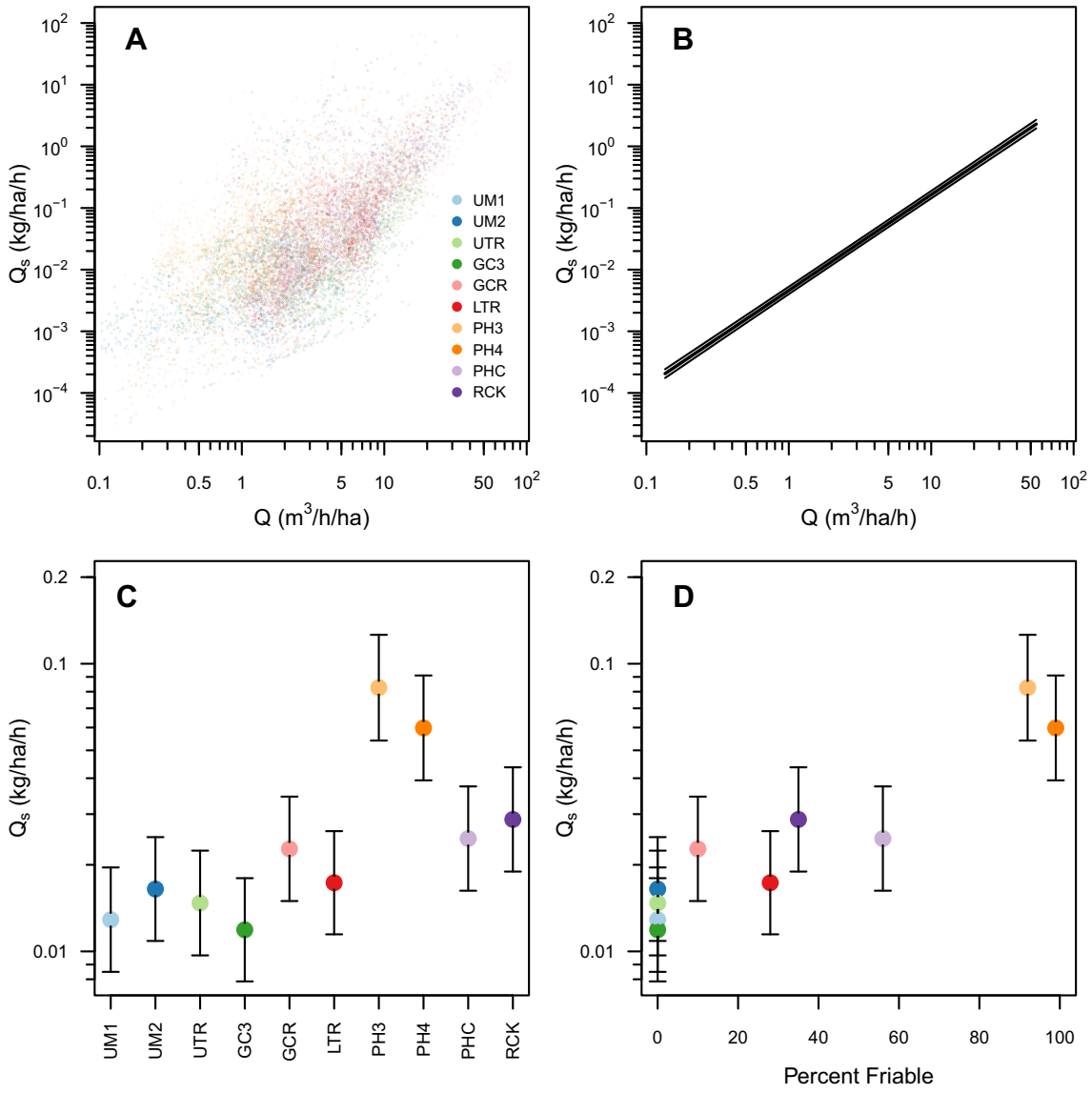

Fig. 5. The all-site statistical analysis (analysis 1A) was conducted to predict suspended sediment yield (SSY; Q_s) as a function of unit discharge (Q). The analysis indicated that discharge, Q, had the largest effect on SSY (B). When year-to-year heterogeneity was accounted for (random effect), site had an additional effect on SSY (C). Generally ordered by watershed (starting with same letter) from upstream (numbered) to downstream for each. See Figs. 1 and 3 for locations. The site effect increased as a function of percent of the watershed composed of the Siletz volcanics, Trask River formation, and landslide deposits (friable; D). The 95% confidence interval for model effects are shown. The error bars correspond to the 95% confidence interval for model effects.

When catchment lithology by area was considered (Figs. 3, 4; Table 2), site-dependent SSY was positively correlated with percent friable watershed area. Specifically, SSY was greater in catchments underlain by Siletz Volcanics ($r = 0.6$), the Trask River Formation ($r = 0.4$), and landslide deposits ($r = 0.9$; Table 4), and displayed an exponential relationship when plotted against percent watershed area underlain by these lithologies, combined (Fig. 5D). In contrast, the site effect had a strong negative correlation with percent area underlain by diabase ($r = -0.7$; Table 4), with the lowest SSY (UM1 and GC3; Table 3) associated with 100% diabase (Table 2), independent of whether or not earthflow terrain was present (present for UM1; absent for GC3).

If absolute α (intercept of Eq. (2)) values (Tables A1, A2) had been considered as a metric of catchment SSY rather than Q_S calculated at the midpoint of other parameter values, the main differences among sites would be consistent. For example, downstream sites RCK and PHC had the highest α (Table A1) and highest site-dependent SSY (Table 3), whereas UTR had the lowest α and lowest site-dependent SSY. Similarly, the upstream sites PH3 and PH4 had the highest α and highest site-dependent SSY (Table 3), whereas UM1 had the lowest α and lowest site-dependent SSY. For upstream sites, β was highest for PH4 (underlain by 100% sedimentary rocks) and lowest for GC3 (underlain by 100% diabase). This indicates a greater ability to transport sediment with increasing Q in the sedimentary catchment (PH4), whereas the sediment supply at the site underlain by diabase (GC3) was exhausted more rapidly as Q increased.

Exceptions to the general correlation between rating curve parameters and site-dependent SSY include GC3 and UM2 that had intermediate α values and relatively low β values (Fig. 7D). This resulted in intermediate Q_s at low Q, but because of the low β, Q_s did not increase dramatically for mid- and high-Q values. These mid- and high-Q values are arguably responsible for moving the most sediment, thus our approach using the mid-point of the

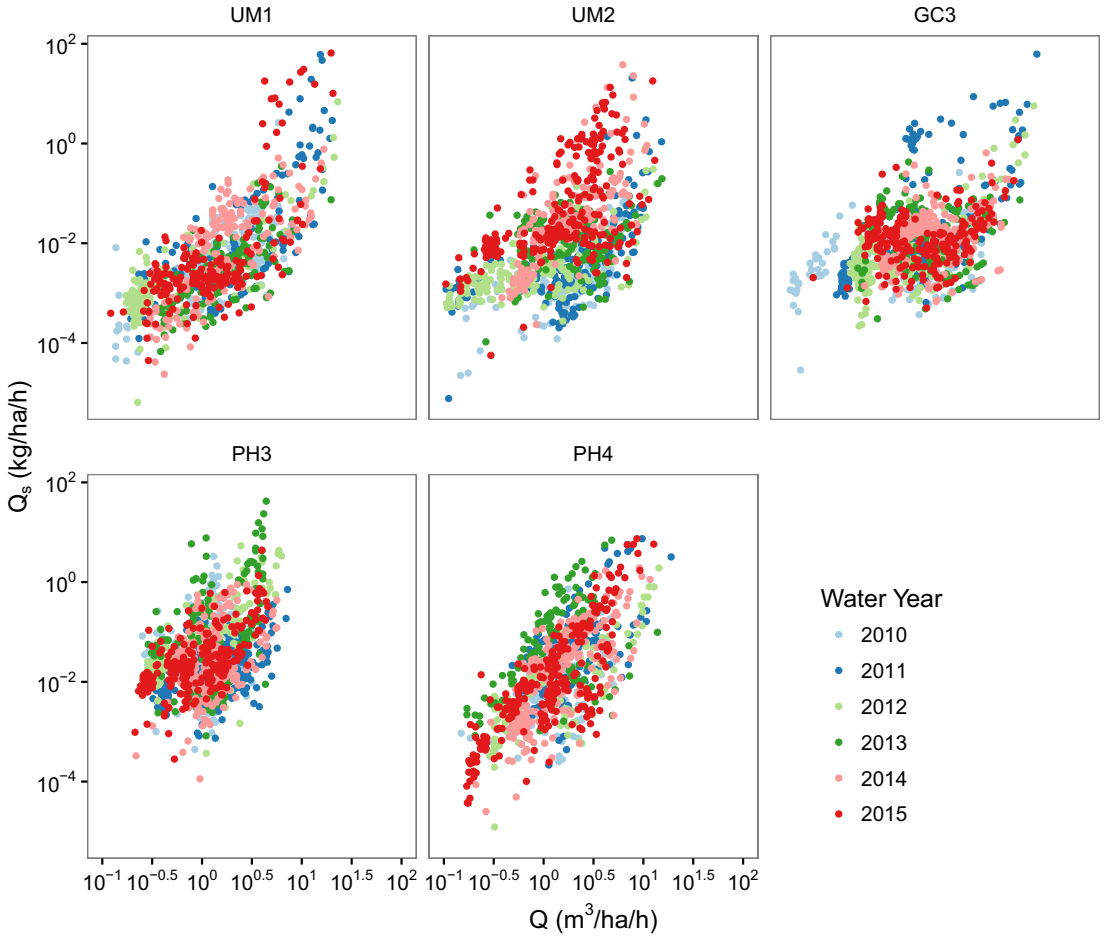

Fig. 6. Suspended sediment yield (Q_s) and discharge (Q) rating curves by water year for each of the upstream sub-catchments. Basis of statistical analysis 2 to assess change in the rating curve by water year while accounting for site differences.

observed range of Q to evaluate site-dependent SSY likely captured the important variations in SSY across sites.

4.2. Forest management effects on suspended sediment transport

Year-to-year variability in SSY was a function of site (i.e., geologic and physiographic setting), as indicated by plausible models (ΔAICc < 4) from statistical analysis 2 (Table A3). Although statistical analysis 1 suggested a site-dependent β, a model including this interaction in the random term was indistinguishable from one including a constant β for upstream sites (Table A3). SSY increased for all sites except PH3 in water year 2011—SSY in UM1, GC3, and PH4 decreased the following year (Fig. 7D). Although roads were built in 2011 in some portions of the study area (Fig. 1), the only subsequent increase in SSY (in water year 2012) was detected in PH3, which did not receive new road construction or upgrades. However, PH3 also had elevated SSY in water years 2012 and 2013 (Fig. 7D) and generally had higher SSY than other sites throughout the study (statistical analysis 1; Fig. 5C). Following harvest (water year 2013), increases in SSY occurred in the harvested catchments PH4, GC3, and UM2 (Fig. 7D). The SSY in both PH4 (clearcut with buffers) and GC3 (clearcut without buffers) declined to pre-harvest levels by water year 2014. Interestingly, the SSY in UM2 (clearcut without buffers) increased annually throughout the post-harvest period, ultimately resulting in the highest SSY of all catchments during the final two years of the study after producing the lowest SSY in the pre-harvest period.

4.3. Catchment setting and physiographic variables

4.3.1. Catchment physiographic variables by site

Catchment physiographic variables (hypsometry, slope, standardized topographic position index (SD TPI), and sediment connectivity (IC)) appeared to be good indicators of the underlying lithology of each site. For example, the hypsometry (distribution of elevation) of PH3, underlain by friable lithologies, was most symmetric, whereas GC3, underlain by 100% diabase, had a pronounced peak at higher elevations (Fig. 8). PH4 was similar to PH3, but had less variance in elevation. UM1, underlain by 100% diabase, but exhibiting earthflow terrain, displayed distinctly bimodal elevation. UM2, underlain by mixed lithology (diabase and sedimentary), had an elevation distribution intermediate between UM1 (diabase) and PH4 (predominantly sedimentary). PH3, PH4, and UM2 had similar, sigmoidal empirical cumulative distribution functions, whereas GC3 and UM1 had near-linear functions. The sigmoidal shape for PH3, PH4, and UM2 indicates intermediate relative elevations are most frequent, with near-equal probabilities of the occurrence of high or low relative elevations. In contrast, a larger proportion of area was at higher elevations for sites underlain by diabase (UM1, GC3) as shown by the greater probabilities of higher elevations for these sites. Furthermore, sites underlain predominantly by diabase had higher mean elevation, variance in elevation, lower skewness, lower kurtosis, and greater relief (~1.8-times greater) compared to others (Table 5).

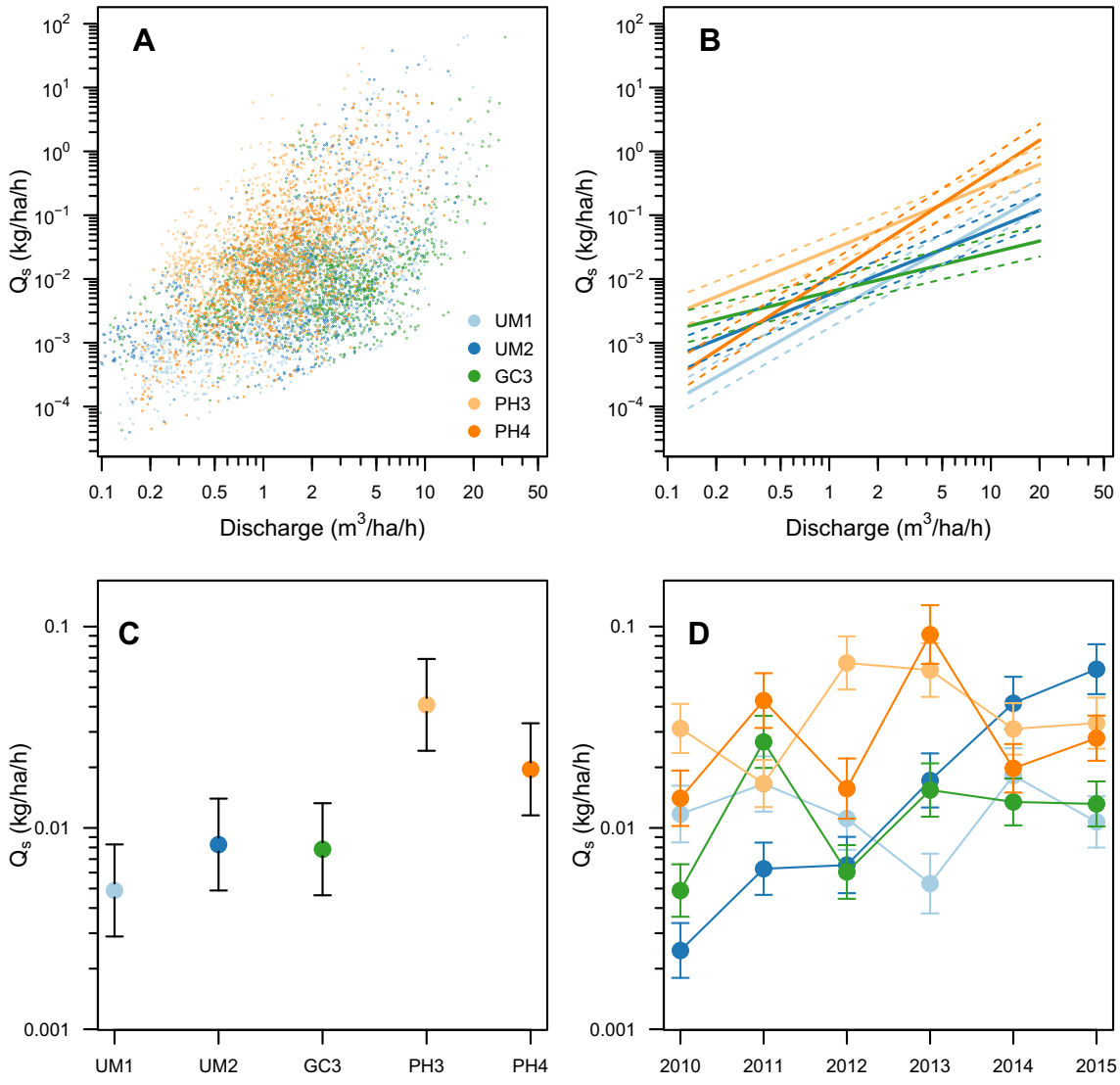

Fig. 7. The analysis using only upstream sub-cathcments (A) indicated a site-dependent Q_s – Q rating curve (B) when year-to-year heterogeneity was accounted for (random effect). However, the average SSY by site (C; ordered east to west; See Figs. 1 and 3 for locations) describes the main differences across mid- and high-range Q values. Site-dependent SSY varied by water year for upstream sub-catchments (D; statistical anlaysis 2). The error bars correspond to the 95% confidence interval for model effects.

Table 3
Effects of Q (m^3 ha^{-1} h^{-1}) and site on Q_s (kg ha^{-1} h^{-1}) when year-to-year heterogeneity by site was accounted for from the all-site analysis (statistical analysis 1A[1,2,3]). See Table A1 for more details.

Site Effect			*Discharge Effect*		
Site	Q_s (kg ha^{-1} h^{-1})	95% CI	Q (m^3 ha^{-1} h^{-1})	Q_s (kg ha^{-1} h^{-1})	95% CI
UM1	0.013	±0.004	0.14	2.0×10^{-4}	$\pm 3.1 \times 10^{-5}$
UM2	0.016	±0.006	0.37	9.7×10^{-4}	$\pm 1.3 \times 10^{-4}$
UTR	0.015	±0.005	1.00	4.6×10^{-3}	$\pm 5.9 \times 10^{-4}$
GC3	0.012	±0.004	2.72	2.1×10^{-2}	$\pm 2.7 \times 10^{-3}$
GCR	0.023	±0.008	7.39	1.0×10^{-1}	$\pm 1.3 \times 10^{-2}$
LTR	0.017	±0.006	20.09	4.8×10^{-1}	$\pm 6.6 \times 10^{-2}$
PH3	0.083	±0.029	54.60	2.3	$\pm 3.4 \times 10^{-1}$
PH4	0.060	±0.021			
PHC	0.025	±0.008			
RCK	0.029	±0.010			

[1] Generalized least squares model.
[2] $\log(Q_s) \sim \log(Q) * \text{Site} + (1|\text{Site:Water Year})$.
[3] AICc = 39914; log-likelihood = −19935; Pseudo-R^2 = 0.63. Deviance = 39870.0 on 11662 residual degrees of freedom.

Table 4
Pearson correlation coefficients between the site effect and lithology (% area). Those with a moderate to strong (±0.4) correlation (Rumsey, 2016) are italicized and those that had a positive correlation with site coefficient are bolded.

	Site Effect	Siletz	Tillamook	Diabase	Dikes/Sills	Yamhill	Trask River
Siletz	***0.6***						
Tillamook	−0.1	0.1					
Diabase	*−0.7*	*−0.7*	*−0.4*				
Dikes/Sills	−0.1	0.1	*1.0*	*−0.4*			
Yamhill	−0.3	−0.2	−0.3	−0.1	−0.3		
Trask River	***0.4***	*0.5*	0.1	I	0.1	*−0.4*	
Landslide	***0.9***	0.3	0.2	*−0.6*	0.2	−0.3	0.1

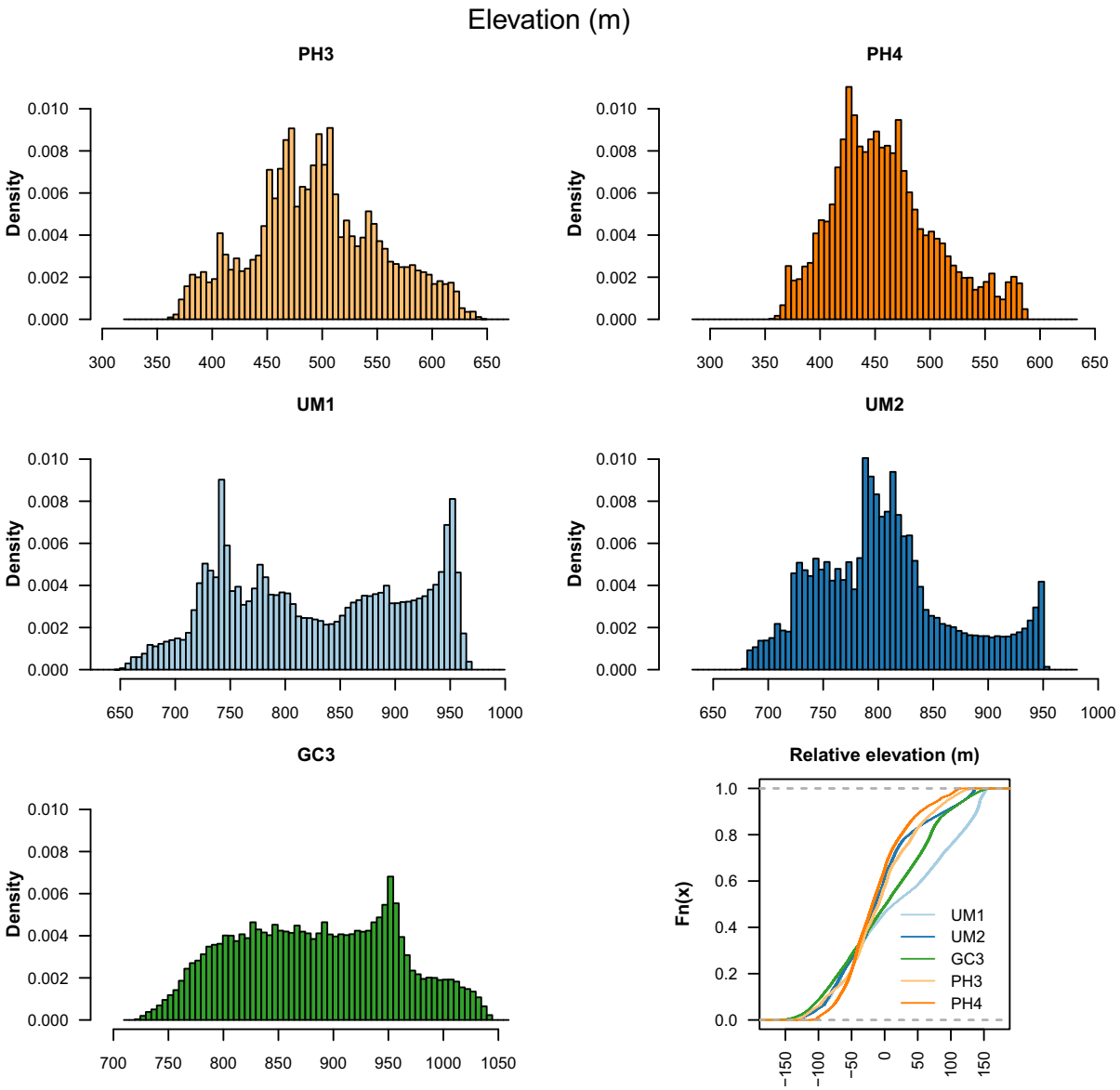

Fig. 8. Elevation (z) distributions and empirical distribution functions for the upstream headwater catchments. PH3 has the most symmetric distribution, and displays an end-member empirical distribution function. Sites underlain by friable or mixed lithologies (PH4; UM2) are more similar to the PH3 distribution than to those underlain by diabase (UM1; GC3).

Slope distributions were also indicative of the underlying lithology of each catchment (Fig. 9). For example, PH3, which is underlain by friable lithologies and exhibits a rotational landslide complex, displayed a right-skewed, bimodal distribution, and greatest variance in slope (Table 5). Slope distributions were most similar for UM2 and PH4, as indicated by their cumulative distribution functions (Fig. 9). The distribution of PH3 was similar to UM2 and PH4 at low slopes, but had a greater proportion of higher slopes (Fig. 9), corresponding to steep head scarps. Catchments with a lithology more resistant to erosion (i.e., UM1, GC3) generally had a greater proportion of their area at higher elevations and typically had steeper slopes. In contrast, catchments with more easily erodible lithologies (i.e., PH3, PH4, UM2) were lower in elevation and had more gentle slopes.

Table 5
Distribution moments for physiographic variables used in the principal component analysis.

Site	Mean	Variance (var)	Skewness (skew)	Kurtosis (kurt)
		Elevation (z)		
UM1	828.2	7048	0.02	1.7
UM2	805.9	3879.7	0.51	2.8
GC3	884.5	5228.3	0.02	2.1
PH3	494.6	3373.9	0.15	2.6
PH4	458.7	2241.3	0.56	2.9
		Slope (%)		
UM1	19.7	9.9	0.3	2.8
UM2	17.3	8.9	0.3	2.4
GC3	21.9	7.3	-0.3	2.9
PH3	20.1	12.2	0.6	2.5
PH4	18.5	9.3	0.6	2.9
		SD TPI		
UM1	0.0055	0.067	-0.43	8.19
UM2	0.0017	0.079	-0.14	7.05
GC3	0.0046	0.029	-0.78	9.07
PH3	-0.0019	0.091	-0.054	5.89
PH4	0.0025	0.086	-0.18	5.25
		IC		
UM1	0.4	0.0053	0.39	4.11
UM2	0.37	0.0045	0.76	5.08
GC3	0.39	0.0038	0.65	4.56
PH3	0.38	0.0069	-0.35	4.73
PH4	0.38	0.0044	0.68	4.83

z = elevation.
SD TPI = standardized topographic position index.
IC = index of connectivity.

The SD TPI metric illustrated the gradation in distribution of roughness across sites (Fig. A1). PH3 had the greatest variance in SD TPI, and lowest kurtosis, whereas GC3 had the lowest variance and greatest kurtosis (Table 5). With decreasing proportion of friable lithologies, the variance of SD TPI decreased, whereas kurtosis increased. This gradation is illustrated in the cumulative distribution function of SD TPI (Fig. A1). As the proportion of the catchment underlain by resistant geology increased (PH3 < PH4 < UM2 < UM1 $\leq$ GC3), the cumulative distribution function increasingly deviated and became more sigmoidal. This analysis of roughness (SD TPI) was conducted over a 10-m window, and thus provides information about mesotopographic variations in topography, such as hummocks and swales. The relatively high variance and low kurtosis for SD TPI in relatively friable catchments (e.g., PH3, PH4) suggests a high proportion of these features, which are correlated to soil and/or sedimentary thickness (Pelletier et al., 2016). Conversely, low variance and high kurtosis in SD TPI indicates fewer such features in sites underlain by resistant diabase (e.g., UM1, GC3). Thus, we can infer that PH3 and PH4 have a greater supply of sediment within their catchments compared to UM1 and GC3 and by extension, UM2 has intermediate sediment supply.

The index of sediment connectivity (IC) exhibited some differences among sites (Fig. A2). The distribution for PH3 was left-skewed, whereas the others were right-skewed (Table 5). UM2, PH3, and PH4 had the greatest kurtosis. Comparatively, UM1 and PH3, which had scarp and slump terrain, had the greatest variance. UM1 and GC3, underlain by diabase, had the greatest mean IC and the lowest α. The lowest mean connectivity was observed for the site with the greatest α (PH3). UM2 displayed characteristics intermediate between PH4 (underlain by sedimentary rocks) and those underlain by resistant diabase (UM1 and GC3).

4.3.2. Physiographic variable analysis

PCA, constructed from the moments of the physiographic variables, indicated the first three components explain >90% of the variance (Table 6). The first PC (PC1; Fig. 10) separated the sites within resistant diabase (UM1 and GC3; positive values) from those located in mixed lithologies (PH4, PH3, UM2; negative values). Positive values of PC1 were correlated with SD TPI kurtosis, elevation variance, mean IC, mean relative elevation, and mean slope. Negative values of PC1 were correlated with skewness of slope, skewness of elevation, SD TPI variance, IC kurtosis, relative elevation kurtosis, and SD TPI skewness (Table 6).

Sites with relatively low SSY and underlain by a resistant lithology (UM1, GC3) plotted in the positive PC1 space of PCA ordination. These sites had low overall SSY (statistical analysis 1), and were resistant to harvest-related increases in SSY (statistical analysis 2), despite road building (UM1, GC3) and harvest without buffers (GC3). In contrast, sites with negative PC1 values were located within weaker, or mixed lithologies and had either higher overall SSY (PH3, PH4; statistical analysis 1), or had harvest-related increases in SSY (UM2, PH4; statistical analysis 2).

The second PC (PC2; Fig. 10A) separated sites with the greatest slump and earthflow terrain (PH3 and UM1; positive values) from those with lower proportions or none (PH3, UM2, and GC3; negative values). Positive PC2 values were associated with greater IC variance, slope variance, and mean IC (Table 6). UM2 and PH4 plotted in a similar region of the PC1-PC2 ordination space. The site within the negative PC1 and positive PC2 field (PH3) had the greatest SSY and had high annual variability in SSY, despite its lack of harvest treatment. The third PC (PC3; Fig. 10B) separated UM sites (UM1, UM2; negative values) from GC3, PH3, and PH4 (positive values). Positive PC3 values were associated with greater mean catchment slope and slope kurtosis, whereas negative values were associated with large relative elevation variance and mean relative elevation (Table 6).

5. Discussion

5.1. Suspended sediment transport by catchment setting

Our results indicated lithology was a first order control over suspended sediment yield (SSY) in the temperate headwater streams studied, with the SSY varying by an order-of-magnitude across the lithologies observed. Catchments underlain by more friable lithologies (e.g., PH3, PH4), such as landslide sediments, sand-

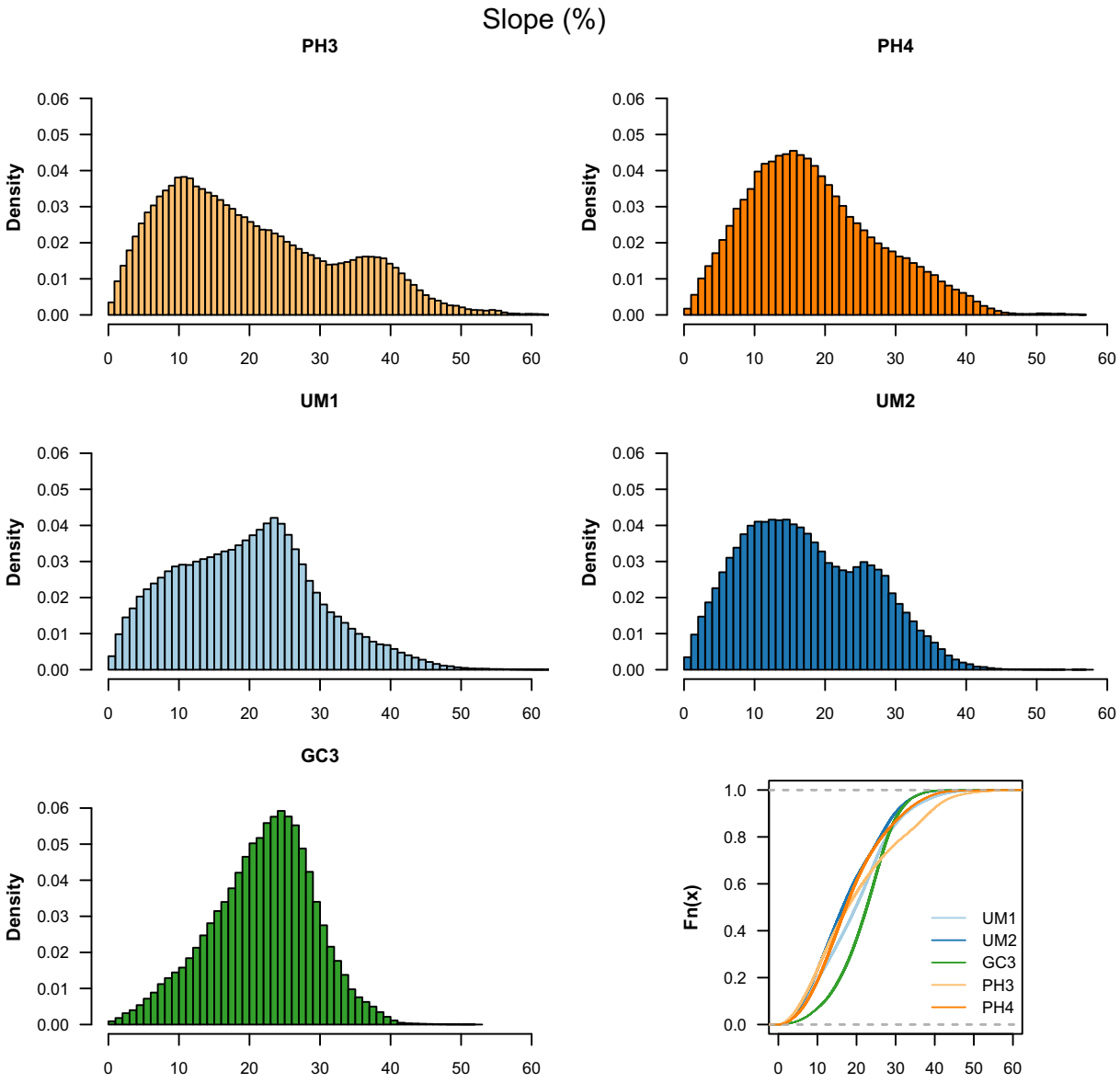

Fig. 9. Slope distributions and empirical distribution functions for upstream headwater catchments. Sites underlain by diabase have one peak at ~25% (UM1; GC3), whereas those underlain by friable or mixed lithologies display right-skewed distributions (PH3, PH4, UM2) and are bimodal if scarps are present (PH3; UM2).

stones and shales, and volcaniclastics generally had the greatest SSY, regardless of land-use activity. Alternatively, catchments that were underlain by resistant lithologies (e.g., UM1, GC3), such as diabase, typically had the lowest SSY during the study. These results are consistent with other studies from diverse regions, including temperate systems in Oregon and California, as well as in the Plains and Rocky Mountains, that have found the magnitude of fluvial sediment yield to be a function of lithology (Colby et al., 1956; Hicks et al., 1996; Kao and Milliman, 2008; Mueller and Pitlick, 2013; O'Connor et al., 2014; Wise and O'Connor, 2016). If lithology is the dominant control on the magnitude of SSY, this could have broad implications for our ability to predict baseline SSY yields, as well as catchment-scale responses to high-flow events and low- to moderate-severity disturbances.

5.2. Forest management effects on suspended sediment transport

Our results provide evidence that temperate, headwater catchments may have differing levels of vulnerability or resilience to increases in SSY following disturbance from forest harvesting activities depending on their lithology. For example, road upgrades appeared to have little impact on SSY for sites underlain by resistant diabase (UM1; GC3), despite previous research that has shown roads to be a principal source of SSY relative to the general harvest area (Beschta, 1978; Grant and Wolff, 1991; Hotta et al., 2007; Swanson and Dyrness, 1975; Tarolli and Sofia, 2016). Similarly, a site that was clearcut *without* riparian buffers (GC3), which was underlain by resistant diabase, had modest increases in SSY in the first year after harvest that was not evident two years later. In contrast, a site that was harvested *with* riparian buffers (PH4), but was underlain by friable rocks, had almost an order-of-magnitude increase in SSY following harvest. Likewise, an unharvested site underlain by friable rocks (PH3) had high year-to-year variability in SSY. Thus, the relative erodibility of contrasting lithologies appears to have influenced the magnitude of SSY response to forest harvesting by controlling sediment supply. This interpretation is additionally supported by the contrasting rating curve β parameter between PH4 (highest β) and GC3 (smallest β),

Table 6
Principal component (PC) cumulative proportion of variance and loadings for the first three components for moments of physiographic variables. Loadings greater than that expected if all variables contributed equally to the variance explained are bolded. See text footnote for variable and moment abbreviations.

	PC1	PC2	PC3
Cumulative Proportion Variance (%)	57.1	84.2	92.8
SD TPI kurt	**0.31**	−0.07	−0.13
z var	**0.29**	0.13	−**0.39**
mean IC	**0.28**	**0.28**	0.01
mean z	**0.27**	0.18	−**0.41**
mean slope	**0.25**	0.11	**0.56**
slope kurt	0.18	−0.10	**0.31**
IC skew	0.03	−**0.47**	−0.25
IC var	−0.11	**0.46**	0.09
slope var	−0.16	**0.44**	0.08
slope skew	−**0.27**	0.23	−0.17
z skew	−**0.28**	−**0.26**	−0.16
SD TPI var	−**0.30**	0.19	−0.19
IC kurt	−**0.30**	−0.09	0.15
z kurt	−**0.31**	−0.18	0.19
SD TPI skew	−**0.32**	0.16	−0.17

z = elevation.
SD TPI = standardized topographic position index.
IC = index of connectivity.
kurt = kurtosis.
var = variance.
skew = skewness.

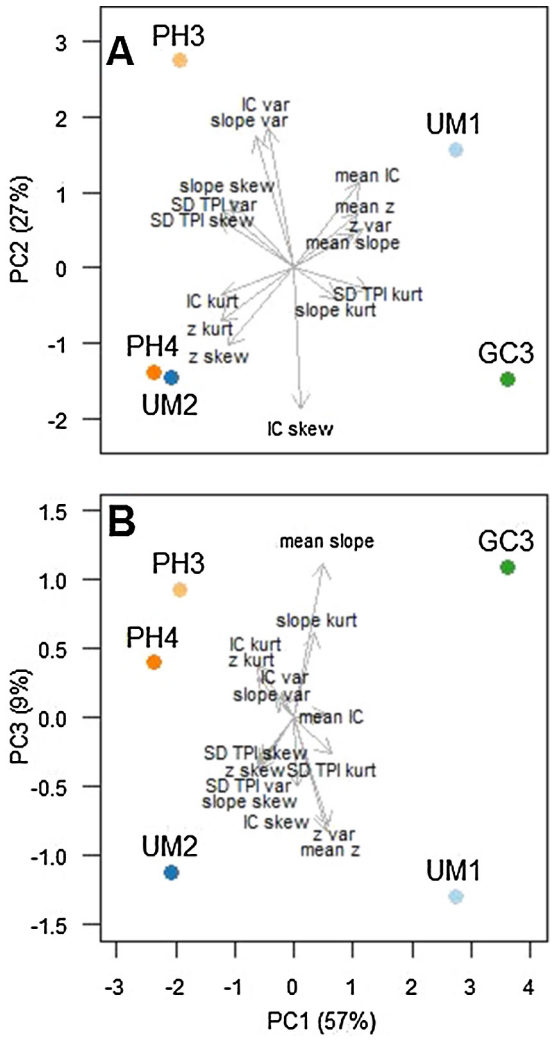

Fig. 10. The first principal component (PC1) (A and B x-axes) explained 57 percent of the variation in physiographic variables between sites. An additional 27 percent of variance in explained by PC2 (A) and 9 percent by PC3 (B). The vectors are proportional to the loadings for each physiographic variable, indicating how each contributes to the principal components.

where the higher β parameter presumably indicates increasing sediment sources with increasing Q (PH4). In contrast, the low β parameter (GC3) indicates constant or limited increases in sediment sources with increasing Q (Sheridan et al., 2011).

While the overall SSY response was predominantly controlled by lithology, the duration of the response to harvest appeared to be dependent on the forest management practice. For instance, PH4 (harvested with buffers) had a large-magnitude increase in SSY following harvest, but the effect was short-lived (one year). In contrast, increased SSY was observed in all years after forest harvest in a site with similar geology and physiographic character to PH4 (UM2), but was harvested without the retention of riparian buffers. Other studies have shown that the general harvest area often contributes little SSY to streams (Hotta et al., 2007; Kreutzweiser and Capell, 2001; Mohr et al., 2013). Rather, the greatest impacts are attributed to linear features, such as roads and skid trails, which can increase sediment connectivity of the landscape to streams (Beschta, 1978; Fredriksen, 1970; Tarolli and Sofia, 2016). Furthermore, riparian buffers are thought to be effective at reducing sediment transport from harvested hillslopes to streams (Broadmeadow and Nisbet, 2004; Gomi et al., 2005). Therefore, the observed increase in SSY in PH4 (harvested with buffers) may have been indirectly related to other harvest activities, rather than transport of sediment through the buffer itself. Once log hauling in the region ceased, SSY returned to pre-harvest levels,. For UM2 (harvested without buffers), increased SSY may have been related to increased ground disturbance or roads, but we cannot definitively link SSY to a specific source.

Our results are consistent with previous studies quantifying the relative contribution of both land-use practices and catchment setting on SSY. In a review of forested headwater streams in the PNW, all sites underlain by erodible sedimentary formations (including the Alsea and Caspar Creek watersheds; n = 13) or volcaniclastic formations (H.J. Andrews Experimental Forest; n = 2) had elevated SSY after forest harvesting, whereas SSY did not increase in sites that were underlain by more resistant metamorphic or intrusive formations after forest harvesting (Gomi et al., 2005). Similarly, several western US watersheds predominantly underlain by resistant basalt had little to no change in suspended sediment concentration following harvest activities, including the Middle Santiam River, Oregon (Sullivan, 1985), Coyote Creek, Oregon (Harr et al., 1979), and Bull Run Watershed, Oregon (Harr and Fredriksen, 1988). The lithologic control on harvest-SSY response has also been observed in other temperate regions such as New Zealand (O'Loughlin and Pearce, 1976).

5.3. Physiographic controls on suspended sediment transport

In this study, catchment physiographic variables varied by dominant catchment lithology, suggesting a correlation between lithology and physiography. This may be an expression of the influence of lithology on both chemical and physical weathering rates (Buss et al., 2017; Portenga and Bierman, 2011), which are responsible for providing eroded material to channels. At large basin scales, physiographic variables have been well correlated with erosion rates (Ahnert, 1970); however, a recent study in Oregon indicated that lithology was a more reliable predictor of erosion and SSY (Wise and O'Connor, 2016).

Comparatively, catchments with erodible lithologies had lower elevations and slopes than more resistant lithologies. We interpret this to be the result of higher rates of erosion in these catchments, which has reduced the higher elevation regions and concentrated

the intermediate elevations. High rates of sediment supply for catchments underlain by easily erodible lithologies (e.g., PH3 and PH4) was further supported by the larger proportion of roughness features (i.e., hummocks and swales), suggesting higher hillslope sediment supply (Pelletier et al., 2016). Alternatively, catchments with the lowest SSY, which were underlain by resistant lithologies (e.g., UM1, GC3), had a greater proportion of their area at high elevations and steeper slopes. These sites (UM1, GC3) also had the greatest mean sediment connectivity, suggesting high transport efficiency and supply-limited conditions, whereas sites with greater sediment supply (i.e., PH3, PH4) were transport-limited. The supply-limited conditions in streams underlain by diabase is further supported by the presence of several bedrock reaches in these streams (UM and GS). In contrast, streams underlain by friable lithologies (PH) are incising into alluvial material in many reaches.

Although we found relationships among catchment lithology, physiographic catchment characteristics, and catchment SSY, the specific sediment sources and delivery processes to the streams are still unclear. While surface roughness has been associated with hillslope erosional processes, such as interill, rill, and gully erosion, this connection has been principally restricted to cultivated, agricultural catchments (Auzet et al., 1995). Forest soils are typically well structured, which promotes infiltration, and limits the potential for infiltration-excess overland flow, even on disturbed forest hillslopes (Litschert and MacDonald, 2009; Wallbrink and Croke, 2002). As such, hillslope erosional processes and contributions of sediment from forested hillslopes are usually minor. However, we argue that the association between catchment physiography and SSY in this case is due to greater availability of hillslope sediment supply, which was likely deposited during previous mass wasting events. Additionally, increases in SSY may be exacerbated by higher rates of in-channel sediment comminution in catchments underlain by friable lithologies. For instance, even though the mass wasting features present in PH are likely inactive, these features are associated with high sediment supply (e.g., landslide toe material), in-channel storage of sediment, and transport capacity (e.g., steep scarps) that would provide high SSY under high flow events. In this case, SSY was elevated even when riparian buffers were retained to mitigate increases in SSY after forest harvesting (PH4). In this unique catchment setting, the greater sediment supply and elevated rate of sediment comminution likely increased the catchment vulnerability to elevated SSY after harvest activities. Additional studies are needed to help clarify the dominant processes driving differential SSY responses across diverse physiography and lithology. Research would benefit by combining SSY measurements with observations/quantification of specific sediment-source erosion through repeat topographic surveys, use of sediment tracer techniques, and/or numerical modelling of terrain evolution.

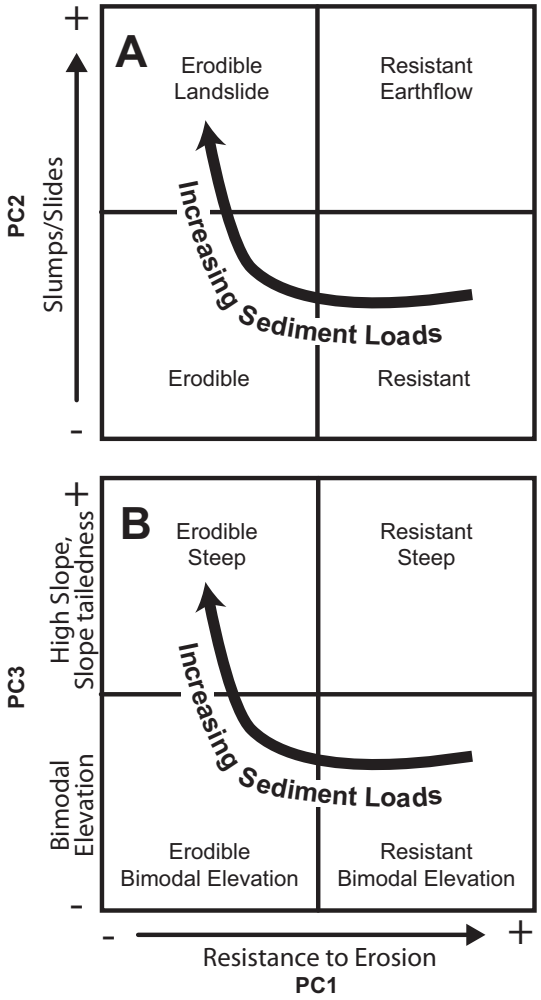

Fig. 11. Interpretation of PCA, where PC1 separates basins underlain by resistant lithologies (positive) from those that are more easily eroded and presumable have higher sediment supplies. PC2 (A) separates sites that display slump and slide terrain (positive) from those that do not. PC3 (B) separates sites with bimodal elevation distributions from those that have higher mean slopes and slope outliers. Relative sediment loads increase with decreasing PC1 values, and increasing PC2 and PC3 values.

6. Conclusion

In this study of temperate, headwater streams, we found that catchment characteristics (lithology and physiography) were a dominant control on suspended sediment yield (SSY) under both unharvested and harvested conditions. Furthermore, we found systematic variations in physiographic variables as a function of lithology, with overall SSY and harvest-related increases in SSY varying with physiographic characteristics. Friable lithologies exhibited higher SSY compared to those underlain by resistant lithologies. The occurrence of harvest-related SSY increases was more dependent upon site characteristics (underlying lithology and physiography) than the specifics of the type of activity (e.g., road building, presence/absence of riparian buffers). We propose that in similar settings, physiographic variables in conjunction with lithology may provide a framework to improve predictions of catchment-scale SSY and land-use impacts on SSY (Fig. 11). Additional research is required to determine the applicability of our findings across broader climatic and geologic settings, as well as across different disturbance regimes.

Acknowledgements

Thanks to two anonymous reviewers and the editors for constructive feedback that improved this manuscript. We thank the Watersheds Research Cooperative (WRC) and associated funders and cooperators (http://watershedsresearch.org/), as well as the Fish and Wildlife Habitat in Managed Forests Research Program for support of this research. This work was partially supported by the USDA National Institute of Food and Agriculture, McIntire Stennis project OREZ-FERM-876. Special thanks to Arne Skaugset, Maryanne Reiter, Sherri Johnson, Amy Simmons, Alex Irving, and Jon Souder for their insight and assistance in data collection, processing, and management. Thanks to Nicholas Cook, Ariel Muldoon, and Jason Dunham for their consultation regarding analyses

conducted in this manuscript. Inquiries regarding data availability can be sent through the director of the WRC (Jon Souder as of submission of manuscript).

Appendix A. Supplementary data

Supplementary data associated with this article can be found, in the online version, at http://dx.doi.org/10.1016/j.jhydrol.2017.03.048.

References

Ahnert, F., 1970. Functional relationships between denudation, relief, and uplift in large, mid-latitude drainage basins. Am. J. Sci. 268, 243–263. http://dx.doi.org/10.2475/ajs.268.3.243.

Akaike, H., 1974. A new look at the statistical model identification. IEEE Trans. Automat. Contr. 19, 716–723. http://dx.doi.org/10.1109/TAC.1974.1100705.

Auzet, A.V., Boiffin, J., Ludwig, B., 1995. Concentrated flow erosion in cultivated catchments: influence of soil surface state. Earth Surf. Process. Landforms 20, 759–767. http://dx.doi.org/10.1002/esp.3290200807.

Bates, D., Maechler, M., Bolker, B., Walker, S., 2015. Fitting linear mixed-effects models using lme4. J. Stat. Softw. 67, 1–48. http://dx.doi.org/10.18637/jss.v067.i01.

Beschta, R.L., 1978. Long-term patterns of sediment production following road construction and logging in the Oregon Coast Range. Water Resour. Res. 14, 1011–1016. http://dx.doi.org/10.1029/WR014i006p01011.

Binkley, D., Brown, T.C., 1993. Forest practices as nonpoint sources of pollution in North America. Water Resour. Bull. 29, 729–740. http://dx.doi.org/10.1111/j.1752-1688.1993.tb03233.x.

Booth, A.M., Roering, J.J., Perron, J.T., 2009. Automated landslide mapping using spectral analysis and high-resolution topographic data: Puget Sound lowlands, Washington, and Portland Hills, Oregon. Geomorphology 109, 132–147. http://dx.doi.org/10.1016/j.geomorph.2009.02.027.

Booth, A.M., Roering, J.J., Rempel, A.W., 2013. Topographic signatures and a general transport law for deep-seated landslides in a landscape evolution model. J. Geophys. Res. Earth Surf. 118, 603–624. http://dx.doi.org/10.1002/jgrf.20051.

Borselli, L., Cassi, P., Torri, D., 2008. Prolegomena to sediment and flow connectivity in the landscape: a GIS and field numerical assessment. Catena 75, 268–277. http://dx.doi.org/10.1016/j.catena.2008.07.006.

Broadmeadow, S., Nisbet, T.R., 2004. The effects of riparian forest management on the freshwater environment: a literature review of best management practice. Hydrol. Earth Syst. Sci. 8, 286–305. http://dx.doi.org/10.5194/hess-8-286-2004.

Brown, G.W., Krygier, J.T., 1971. Clear-cut logging and sediment production in the Oregon Coast Range. Water Resour. Res. 7, 1189–1198. http://dx.doi.org/10.1029/WR007i005p01189.

Brown, T.C., Binkley, D., 1994. Effect of management on water quality in North American forests. USDA For. Serv. Gen. Tech. Rep. RM-248, 1–27.

Burnham, K., Anderson, D., 2002. Model Selection and Multimodel Inference: A Practical Information-Theoretic Approach. Springer, New York, pp. 1–487.

Burns, S.F., Burns, W.J., Hinkle, J.C., James, D.H., 2006. Landslides geohazard map for Portland, Oregon, USA [WWW Document]. IAEG2006. URL http://iaeg2006.geolsoc.org.uk/cd/.

Buss, H.L., Chapela Lara, M., Moore, O.W., Kurtz, A.C., Schulz, M.S., White, A.F., 2017. Lithological influences on contemporary and long-term regolith weathering at the Luquillo Critical Zone Observatory. Geochim. Cosmochim. Acta 196, 224–251. http://dx.doi.org/10.1016/j.gca.2016.09.038.

Carson, M.A., 1976. Mass-wasting, slope development and climate. In: Geomorphology and Climate. John Wiley and Sons, New York, pp. 101–136.

Cavalli, M., Tarolli, P., Marchi, L., Dalla Fontana, G., 2008. The effectiveness of airborne LiDAR data in the recognition of channel-bed morphology. Catena 73, 249–260. http://dx.doi.org/10.1016/j.catena.2007.11.001.

Cavalli, M., Trevisani, S., Comiti, F., Marchi, L., 2013. Geomorphometric assessment of spatial sediment connectivity in small Alpine catchments. Geomorphology 188, 31–41. http://dx.doi.org/10.1016/j.geomorph.2012.05.007.

Church, M., 2002. Geomorphic thresholds in riverine landscapes. Freshw. Biol. 47, 541–557. http://dx.doi.org/10.1046/j.1365-2427.2002.00919.x.

Colby, B.R., Hembree, C.H., Rainwater, F.H., 1956. Sedimentation and chemical quality of surface waters in the Wind River Basin, Wyoming. Geol. Surv. Water-Supply Pap. 1373, 1–336.

Cooley, S.W., 2015. GIS4Geomorphology [WWW Document]. URL http://www.gis4geomorphology.com (accessed 1.1.16).

Crema, S., Schenato, L., Goldin, B., Marchi, L., Cavalli, M., 2015. Toward the development of a stand-alone application for the assessment of sediment connectivity. Rend. Online Soc. Geol. Ital. 34, 58–61. http://dx.doi.org/10.33.01/ROL.2015.37.

Croke, J.C., Hairsine, P.B., 2006. Sediment delivery in managed forests: a review. Environ. Rev. 14, 59–87. http://dx.doi.org/10.1139/a05-016.

Desilets, S.L.E., Nijssen, B., Ekwurzel, B., Ferré, T.P.A., 2007. Post-wildfire changes in suspended sediment rating curves: Sabino Canyon. Arizona. Hydrol. Process. 21, 1413–1423. http://dx.doi.org/10.1002/hyp.6352.

Fredriksen, R.L., 1970. Erosion and sedimentation following road construction and timber harvest on unstable soils in three small western Oregon watersheds. USDA For. Serv. Res. Pap. PNW-104, 1–15.

Gomi, T., Moore, Dan., Moore, R.D., Hassan, M.A., 2005. Suspended sediment dynamics in small forest streams of the Pacific Northwest. J. Am. Water Resour. Assoc. 41, 877–898. http://dx.doi.org/10.1111/j.1752-1688.2005.tb03775.x.

Grant, G.E., Wolff, A.L., 1991. Long-term patterns of sediment transport following timber harvest, Western Cascade Mountains, Oregon. Sediment Streamwater Qual. a Chang. Environ. Trends Expl. IAHS 203, 31–41.

Harr, R.D., Fredricksen, R.L., Rothacher, J., 1979. Changes in streamflow following timber harvest in southwestern Oregon. USFA For. Serv. Pap. PNW-249, 1–22.

Harr, R.D., Fredriksen, R.L., 1988. Water quality after logging small watersheds within the Bull Run Watershed. Oregon. Water Resour. Bull. 24, 1103–1111. http://dx.doi.org/10.1111/j.1752-1688.1988.tb03027.x.

Haynes, R.W., 2003. An analysis of the timber situation in the United States: 1952 to 2050. Gen. Tech. Rep. PNW-GTR-56, 254 p.

Hicks, D., Hill, J., Shankar, U., 1996. Variation of suspended sediment yields around New Zealand: the relative importance of rainfall and geology. Eros. Sediment Yield Glob. Reg. Perspect IAHS 236, 149–156.

Highland, L.M., Bobrowsky, P., 2008. The landslide handbook—A guide to understanding landslides [WWW Document]. USGS Circ. 1325. URL https://pubs.usgs.gov/circ/1325/.

Hotta, N., Kayama, T., Suzuki, M., 2007. Analysis of suspended sediment yields after low impact forest harvesting. Hydrol. Process. 21, 3565–3575. http://dx.doi.org/10.1002/hyp.

Jenness, J., Beier, P., Brost, B., 2013. Land facet corridor designer: extension for ArcGIS [WWW Document]. URL http://www.jennessent.com/arcgis/land_facets.htm.

Johnstone, S.A., Hilley, G.E., 2014. Lithologic control on the form of soil-mantled hillslopes. Geology 43, 83–86. http://dx.doi.org/10.1130/G36052.1.

Kao, S.J., Milliman, J.D., 2008. Water and sediment discharge from small mountainous rivers, Taiwan: the roles of lithology, episodic events, and human activities. J. Geol. 116, 431–448. http://dx.doi.org/10.1086/590921.

Kemp, P., Sear, D., Collins, A., Naden, P., Jones, I., 2011. The impacts of fine sediment on riverine fish. Hydrol. Process. 25, 1800–1821. http://dx.doi.org/10.1002/hyp.7940.

Klein, R.D., Lewis, J., Buffleben, M.S., 2012. Logging and turbidity in the coastal watersheds of northern California. Geomorphology 139–140, 136. http://dx.doi.org/10.1016/j.geomorph.2011.10.011.

Kreutzweiser, D.P., Capell, S.S., 2001. Fine sediment deposition in streams after selective forest harvesting without riparian buffers. Can. J. For. Res. 31, 2134–2142. http://dx.doi.org/10.1139/x02-086.

Langbein, W.B., 1947. Topographic characteristics of drainage basins. Geol. Surv. Water-Supply Pap.. 968-C, 1-156.

Legendre, P., Legendre, L., 1998. Numerical ecology. In: Developments in Environmental Modelling. Elsevier, Amsterdam. http://dx.doi.org/10.1017/CBO9781107415324.004, p. 853.

Leopold, L.B., Wolman, M.G., Miller, J.P., 1964. Fluvial Processes in Geomorphology. Dover Publications Inc, New York.

Lewis, J., Eads, R., 2009. Implementation guide for turbidity threshold sampling: Principles, procedures, and analysis. Gen. Tech. Rep. U.S. Department of Agriculture, Forest Service, Pacific Southwest Research Station, Albany, CA.

Litschert, S.E., MacDonald, L.H., 2009. Frequency and characteristics of sediment delivery pathways from forest harvest units to streams. For. Ecol. Manage. 259, 143–150. http://dx.doi.org/10.1016/j.foreco.2009.09.038.

Macdonald, J.S., Beaudry, P.G., MacIsaac, E.A., Herunter, H.E., 2003. The effects of forest harvesting and best management practices on streamflow and suspended sediment concentrations during snowmelt in headwater streams in sub-boreal forests of British Columbia, Canada. Can. J. For. Res. 33, 1397–1407. http://dx.doi.org/10.1139/x03-110.

Majka, D., Jenness, J., Beier, P., 2007. CorridorDesigner: ArcGIS tools for designing and evaluating corridors.

Marshall, M.S., 2016. Slope Failure Eetection Through Multi-Temporal Lidar Data and Geotechnical Soils Analysis of the Deep-Seated Madrone Landslide, Coast Range. Portland State University, Oregon.

Mazerolle, M.J., 2015. AICcmodavg: model selection and multimodel inference based on (Q)AIC(c). R Packag. version 2.0-3.

McKean, J., Nagel, D., Tonina, D., Bailey, P., Wright, C.W., Bohn, C., Nayegandhi, A., 2009. Remote sensing of channels and riparian zones with a narrow-beam aquatic-terrestrial LIDAR. Remote Sens. 1, 1065–1096. http://dx.doi.org/10.3390/rs1041065.

McKean, J., Roering, J., 2004. Objective landslide detection and surface morphology mapping using high-resolution airborne laser altimetry. Geomorphology 57, 331–351. http://dx.doi.org/10.1016/S0169-555X(03)00164-8.

Miller, M.B., 2014. Roadside Geology of Oregon. Mountain Press Publishing Company, Missoula, MT, pp. 1–386.

Milliman, J.D., Farnsworth, K.L., Albertin, C.S., 1999. Flux and fate of fluvial sediments leaving large islands in the East Indies. J. Sea Res. 41, 97–107. http://dx.doi.org/10.1016/S1385-1101(98)00040-9.

Milliman, J.D., Meade, R.H., 1983. World-wide delivery of river sediment to the oceans. J. Geol. 91, 1–21.

Milliman, J.D., Syvitski, J.P.M., 1992. Geomorphic/tectonic control of sediment discharge to the ocean: the importance of small mountainous rivers. J. Geol. 100, 525–544.

Mohr, C.H., Coppus, R., Iroumé, A., Huber, A., Bronstert, A., 2013. Runoff generation and soil erosion processes after clear cutting. J. Geophys. Res. Earth Surf. 118, 814–831. http://dx.doi.org/10.1002/jgrf.20047.
Montgomery, D.R., 2007. Is agriculture eroding civilization's foundation? GSA Today 17, 1–4. http://dx.doi.org/10.1130/GSAT01710A.1.
Montgomery, D.R., 1999. Process domains and the river continuum. J. Am. Water Resour. Assoc. 35, 397–410. http://dx.doi.org/10.1111/j.1752-1688.
Montgomery, D.R., Brandon, M.T., 2002. Topographic controls on erosion rates in tectonically active mountain ranges. Earth Planet. Sci. Lett. 201, 481–489. http://dx.doi.org/10.1016/S0012-821X(02)00725-2.
Montgomery, D.R., Buffington, J.M., 1997. Channel-reach morphology in mountain drainage basins. Bull. Geol. Soc. Am. 109, 596–611. http://dx.doi.org/10.1130/0016-7606(1997) 109<0596:CRMIMD>2.3.CO;2.
Moody, J.A., Martin, D.A., Cannon, S.H., 2008. Post-wildfire erosion response in two geologic terrains in the western USA. Geomorphology 95, 103–118. http://dx.doi.org/10.1016/j.geomorph.2007.05.011.
Mueller, E.R., Pitlick, J., 2013. Sediment supply and channel morphology in mountain river systems: 1. Relative importance of lithology, topography, and climate. J. Geophys. Res. Earth Surf. 118, 2325–2342. http://dx.doi.org/10.1002/2013JF002843.
Mueller, E.R., Smith, M.E., Pitlick, J., 2016. Lithology-Controlled Evolution of Stream Bed Sediment and Basin-Scale Sediment Yields in Adjacent Mountain Watersheds. Earth Surf. Process. Landforms, Idaho, USA. 10.1002/esp.3955.
O'Byrne, T.N., 1967. A correlation of rock types with soils, topography, and erosion in the Gisborne-East Cape region. New Zeal. J. Geol. Geophys. 10, 217–231. http://dx.doi.org/10.1080/00288306.1967.10428192.
O'Connor, J.E., Mangano, J.F., Anderson, S.W., Wallick, J.R., Jones, K.L., Keith, M.K., 2014. Geologic and physiographic controls on bed-material yield, transport, and channel morphology for alluvial and bedrock rivers, western Oregon. Bull. Geol. Soc. Am. 126, 377–397. http://dx.doi.org/10.1130/B30831.1.
O'Loughlin, C.L., Pearce, A.J., 1976. Influence of Cenozoic geology on mass movement and sediment yield response to forest removal, North Westland, New Zealand. Bull. Int. Assoc. Eng. Geol. 13, 41–46. http://dx.doi.org/10.1007/BF02634757.
Oregon Lidar Consortium, 2012. Central Coast Study Area. Oregon Department of Geology and Mineral Industries Lidar Program Data, Portland, Oregon. http://dx.doi.org/10.5069/G9QC01D1.
Paustian, S.J., Beschta, R.L., 1979. The suspended sediment regime of an Oregon Coast Range stream. J. Am. Water Resour. Assoc. 15, 144–154. http://dx.doi.org/10.1111/j.1752-1688.1979.tb00295.x.
Pelletier, J.D., Broxton, P.D., Hazenberg, P., Zeng, X., Trock, P.A., Niu, G.-Y., Williams, Z., Brunke, M.A., Gochis, D., 2016. A gridded global data set of soil, intact regolith, and sedimentary deposit thicknesses for regional and global land surface modeling. J. Adv. Model. Earth Syst. 8, 1–25. http://dx.doi.org/10.1002/2013MS000282.
Portenga, E.W., Bierman, P.R., 2011. Understanding Earth's eroding surface with 10Be. GSA Today 21, 4–10. http://dx.doi.org/10.1130/G111A.1.
Prestemon, J.P., Wear, D.N., Foster, M.O., 2015. The global position of the U.S. forest products industry. U.S. Dep. Agric. For. Serv. South. Res. Stn. e-General Tech. Rep. SRS-204. 1-24.
R Development Core Team, 2015. R: A language and environment for statistical computing.
Redwood Sciences Laboratory, 2016. Sediment laboratory procedures. USDA Forest Service.
Reiter, M., Heffner, J.T., Beech, S., Turner, T., Bilby, R.E., 2009. Temporal and spatial turbidity patterns over 30 years in a managed forest of western Washington. J. Am. Water Resour. Assoc. 45, 793–808. http://dx.doi.org/10.1111/j.1752-1688.2009.00323.x.
Roman, D.C., Vogel, R.M., Schwarz, G.E., 2012. Regional regression models of watershed suspended-sediment discharge for the eastern United States. J. Hydrol. 472–473, 53–62. http://dx.doi.org/10.1016/j.jhydrol.2012.09.011.
Rumsey, D.J., 2016. Statistics for dummies. Wiley, 1–408.
Schwarz, G.E., Alexander, R.B., 1995. Soils data for the conterminous United States derived from the NRCS State Soil Geographic (STATSGO) Data Base [WWW Document]. URL https://water.usgs.gov/GIS/metadata/usgswrd/XML/ussoils.xml.
Sheridan, G.J., Lane, P.N.J., Sherwin, C.B., Noske, P.J., 2011. Post-fire changes in sediment rating curves in a wet Eucalyptus forest in SE Australia. J. Hydrol. 409, 183–195. http://dx.doi.org/10.1016/j.jhydrol.2011.08.016.
Sofia, G., Marinello, F., Tarolli, P., 2016. Metrics for quantifying anthropogenic impacts on geomorphology: road networks. Earth Surf. Process. Landforms 41, 240–255. http://dx.doi.org/10.1002/esp.3842.
Soil survey of Tillamook County, Oregon [WWW Document], 2013. URL https://www.nrcs.usda.gov/Internet/FSE_MANUSCRIPTS/oregon/tillamookOR2013/TillamookOR.pdf.
Strahler, A.N., 1952. Hypsometric (area-altitude) analysis of erosional topography. Geol. Soc. Am. Bull. 63, 1117–1142.
Sullivan, K., 1985. Long-term patterns of water quality in a managed watershed in Oregon: 1. Suspended sediment. Water Resour. Bull. 21, 977–987.
Surfleet, C.G., Skaugset, A.E., 2013. The effect of timber harvest on summer low flows, Hinkle Creek, Oregon. West. J. Appl. For. 28, 13–21. http://dx.doi.org/10.5849/wjaf.11-038.
Suttle, K.B., Power, M.E., Levine, J.M., McNeely, C., 2004. How fine sediment in riverbeds impairs growth and survival of juvenile salmonids. Ecol. Appl. 14, 969–974. http://dx.doi.org/10.1890/03-5190.
Swanson, F.J., Dyrness, C.T., 1975. Impact of clear-cutting and road construction on soil erosion by landslides in the western Cascade Range. Oregon. Geol. 0–3. http://dx.doi.org/10.1130/0091-7613(1975) 3<393:IOCARC>2.0.CO;2.
Syvitski, J.P., Morehead, M.D., Bahr, D.B., Mulder, T., 2000. Estimating fluvial sediment transport: the rating parameters. Water Resour. Res. 36, 2747–2760. http://dx.doi.org/10.1029/2000WR900133.
Syvitski, J.P.M., Milliman, J.D., 2007. Geology, geography, and humans battle for dominance over the delivery of fluvial sediment to the coastal ocean. J. Geol. 115, 1–19. http://dx.doi.org/10.1086/509246.
Tarolli, P., Sofia, G., 2016. Human topographic signatures and derived geomorphic processes across landscapes. Geomorphology 255, 140–161. http://dx.doi.org/10.1016/j.geomorph.2015.12.007.
Tremblay, A., 2015. LMERConvenienceFunctions: model selection and post-hoc analysis for (G)LMER models. R Packag. version 2, 10.
Turner, T., Ward, J., James, P., Reiter, M., 2007. Utilization of LIDAR-derived topographic data for landform mapping and slope stability analysis, in: Cordilleran Section - 103rd Annual Meeting (4–6 May 2007).
United States Environmental Protection Agency, 2016. National summary of impaired waters and TMDL [WWW Document]. URL https://iaspub.epa.gov/waters10/attains_index.home, Date accessed: July 14, 2016.
USGS, 2014. Geologic Units in Tillamook County, Oregon [WWW Document]. Miner. Resour. on-line Spat. data, URL. http://mrdata.usgs.gov/geology/state/fips-unit.php?code=f41057.
Wallbrink, P.J., Croke, J., 2002. A combined rainfall simulator and tracer approach to assess the role of Best Management Practices in minimising sediment redistribution and loss in forests after harvesting. For. Ecol. Manage. 170, 217–232. http://dx.doi.org/10.1016/S0378-1127(01)00765-4.
Warrick, J.A., Rubin, D.M., 2007. Suspended-sediment rating curve response to urbanization and wildfire, Santa Ana River, California. J. Geophys. Res. Earth Surf. 112, 1–15. http://dx.doi.org/10.1029/2006JF000662.
Wells, R.E., Snavely, P.D., J., MacLeod, N.S., Kelly, M.M., Parker, M.J., 1994. Geologic map of the Tillamook Highlands, Northwest Oregon Coast Range. Open-File Rep. 94–21 24 and 2 sheets.
Whipple, K.X., Tucker, G.E., 1999. Dynamics of the stream-power river incision model: Implications for height limits of mountain ranges, landscape response timescales, and research needs. J. Geophys. Res. 104, 17661–17664.
Wise, D.R., O'Connor, J., 2016. A spatially explicit suspended-sediment load model for Western Oregon. U.S. Geol. Surv. Sci. Investig. Rep. 2016–507, 1–25.
Wobus, C., Whipple, K.X., Kirby, E., Snyder, N., Johnson, J., Spyropolou, K., Crosby, B., Sheehan, D., 2006. Tectonics from topography: procedurses, promise, and pitfalls. Geol. Soc. Am. Spec. Pap. 398, 55–74. http://dx.doi.org/10.1130/2006.2398(04).
Wong, B.B.-L., 1999. Controls on Movement of Selected Landslides in the Coast Range and Western Cascades. Oregon State University, Oregon.
Wood, P., Armitage, P., 1997. Biological effects of fine sediment in the lotic environment. Environ. Manage. 21, 203–217. http://dx.doi.org/10.1007/s002679900019.
Zuur, A.F., Ieno, E.N., Walker, N.J., Saveliev, A.A., Smith, G.M., 2009. Mixed effects models and extensions in ecology with R. In: Gail, M., Krickeberg, K., Samet, J.M., Tsiatis, A., Wong, W. (Eds.), Statistics for Biology and Health. Springer, New York, pp. 1–574. http://dx.doi.org/10.1016/B978-0-12-387667-6.00013-0.
Zybach, B., 2003. The great fires: Indian burning and catastrophic forest fire patterns of the Oregon Coast Range, 1491-1951. Oregon State University.